Transactions on Machine Intelligence 7(2) (2024) 107-135

ISSN Online: 2821-1693

Transactions on Machine Intelligence

Journal Homepage: https://tmachineintelligence.ir/index.php/TMI

Control of Vehicle Active Suspension System Using Neural Network

S. Z. Ahmadi SheykhShabani [1,*], D. Sheikhi [2]

[1] Masters Student, Control Engineering, Iran University of Science and Technology, Tehran, Iran.
[2] Masters Student, Control Engineering, Iran University of Science and Technology, Tehran, Iran

ARTICLE INFO

Article History:
Received 7 March 2024
Received in revised form 13 April 2024
Accepted 5 June 2024
Available online 18 June 2024

Keywords:
Control Vibration, Active Suspension, Neural Network, Neural Controller

ABSTRACT

The primary cause of vehicle vibration stems from road irregularities. Addressing this, an effective strategy involves implementing a robust artificial neural network control system to manage the vehicle suspension system's vibrations. To achieve comprehensive vibration control for the entire suspension system, a robust neural network-based control system is employed. The complete vehicle system operates with 7 degrees of freedom, encompassing vertical axis motion, angular variations around the X axis, and angular changes around the Y axis of the car chassis. The proposed control system integrates a robust controller, a neural controller, and a neural network model tailored for the vehicle suspension system. To assess simulation outcomes, a proportional integral derivative (PID) controller is utilized for overall vehicle suspension system vibration control. The study introduces random road roughness as a disturbance factor applied to the proposed control system. Simulation results affirm that the suggested neural control system demonstrates highly effective control performance, with minimal error in adapting to unexpected road disturbances affecting the vehicle suspension.

1. INTRODUCTION

In recent studies, novel approaches have been proposed to enhance the performance of electromagnetic suspension systems and active suspension systems in vehicles. Liu et al. (2021) introduced a neural network-based adaptive event trigger control for electromagnetic suspension systems, aiming to reduce communication burden and ensure optimal vertical displacement and speed, preventing Zeno behavior [1]. Li et al. (2022) explored an active suspension control strategy utilizing a particle swarm-optimized fuzzy neural network, achieving significant improvements in vehicle driving performance compared to passive suspension and PID-controlled active suspension systems [2]. Additionally, Liu et al. (2020) presented an adaptive neural network controller for active suspension systems with hydraulic actuators, contributing to enhanced ride comfort and overall ride quality [3].

Today, the escalating demand for enhanced security, comfort, and trust in vehicles has become an integral consideration for system designers. Technological advancements and the pursuit of driving comfort have led automotive manufacturers to widely incorporate active suspension systems in their vehicles. Particularly prevalent in the passenger car industry, these systems have significantly elevated comfort levels and overall vehicle

* Corresponding Author: zohreahmadi9574@gmail.com
Masters Student, Control Engineering, Iran University of Science and Technology, Tehran, Iran.

http://dx.doi.org/10.47176/TMI.2024.107

maintenance under diverse driving and road conditions. While initially implemented in large-scale luxury cars, the potential advantages, efficiency, and performance of active suspension systems make them particularly suitable for small passenger cars and non-road vehicles.

Active suspension systems employ hydraulic or pneumatic actuators strategically placed parallel to the spring and damper to precisely control vehicle vibrations. These systems utilize information gathered from body vibrations to apply an optimal control approach. The design of active car suspension systems has been a focal point of global automotive industry research. This study addresses various car models, including 1/4, 1/2, and full car models, with an emphasis on optimizing parameters like body displacement, suspension system displacement, body acceleration, braking-induced internal disturbances, and axle forces. Notably, acceleration to the body and suspension system displacement takes precedence in optimization efforts due to their direct impact on passenger comfort and system displacement. Understanding the non-linear behavior of hydraulic actuators is crucial, as scientific tests underscore its significance in determining the appropriate compromise for an effective car suspension system.

The car's suspension system, an integral part of its chassis, plays a crucial role in connecting with all lower components. Beyond providing passenger comfort, it significantly contributes to the car's stability, adhesion, and balance on the road. High-performance cars like Porsche Boxster, Mustang, and Dodge Challenger owe their exceptional balance and road grip to advanced active suspension systems.Apart from supporting the car's weight, the suspension system must adeptly absorb road shocks, preventing their transfer to the car body. Additionally, it should effectively dampen fluctuations induced by uneven surfaces, designed to ensure tire contact with the road in various conditions.

Innovative approaches by researchers include suggesting a flexible and model-free control structure based on vehicle insights and semi-active suspension dynamics [4]. Reference [5] introduces a load-dependent controller design to address multi-objective control challenges in the vehicle's active suspension system using linear matrix inequalities. Reference [6] delves into the H_∞ robust control problem for active vehicle suspension systems, considering operator time delays. Lastly, reference [7] proposes a method for designing static output feedback controllers and robust static feedback H_∞ controllers for active vehicle suspensions, leveraging linear matrix inequalities and genetic algorithms.

Reference [8] explores the vibration control performance of an electrorheological seat suspension system using a robust sliding mode controller. In reference [9], the overall performance of a semi-active suspension control system for a truck is discussed. Spectral analysis methods are employed in reference [10] to accurately calculate root mean square values for control forces, suspension wear, and vehicle tire deflection in the front and rear of a semi-car model. Reference [11] investigates the vibration control performance of the seat suspension system of a nonlinear model for a complete car using a fuzzy logic controller. A multi-law optimization method for designing mechatronic vehicles with active suspension is detailed in reference [12], utilizing the neural network control method to control the seat suspension system of a complete nonlinear car model. Reference [13] conducts about using a neural network controller to reduce the seat vibrations of a non-linear full vehicle model that has a permanent magnet synchronous motor (PMSM) actuator in its active suspension system. The authors propose a back-propagation algorithm to train the neural network controller and compare its performance with a conventional PID controller. Reference [14] conducts research on the vertical vibrations of a vehicle using a neural network. Reference [15] designs a movable arm suspension system to reduce horizontal rotation and impulses caused by the vehicle. In reference [16], a semi-active control system for a vehicle suspension system with a magnetic damper is presented. Reference [17] outlines an approach for designing active and passive car suspension systems with the aim of maximizing passenger comfort. Reference [18] presents an approach for the design of vehicle suspension systems, and reference [19] conducts research on the sliding mode control of active suspensions for a complete car model.

In this paper, a resilient control system based on a resilient neural network is introduced to manage the vibration of the entire vehicle. The complete vehicle suspension model is first presented under desired conditions. Subsequently, the proposed control system and the integral proportional controller of the derivative are designed. The results obtained from the neural network-based control system and the integral proportional controller are then discussed and compared. Finally, the simulation results are used to evaluate the performance and efficiency of the proposed control method, and conclusions are presented.

2. MODEL OF ACTIVE SUSPENSION SYSTEM

To characterize the vertical dynamics of a vehicle traveling at a constant speed on an irregular road, the mathematical model employed is that of a vehicle with 7 degrees of freedom, as illustrated in Figure 1.

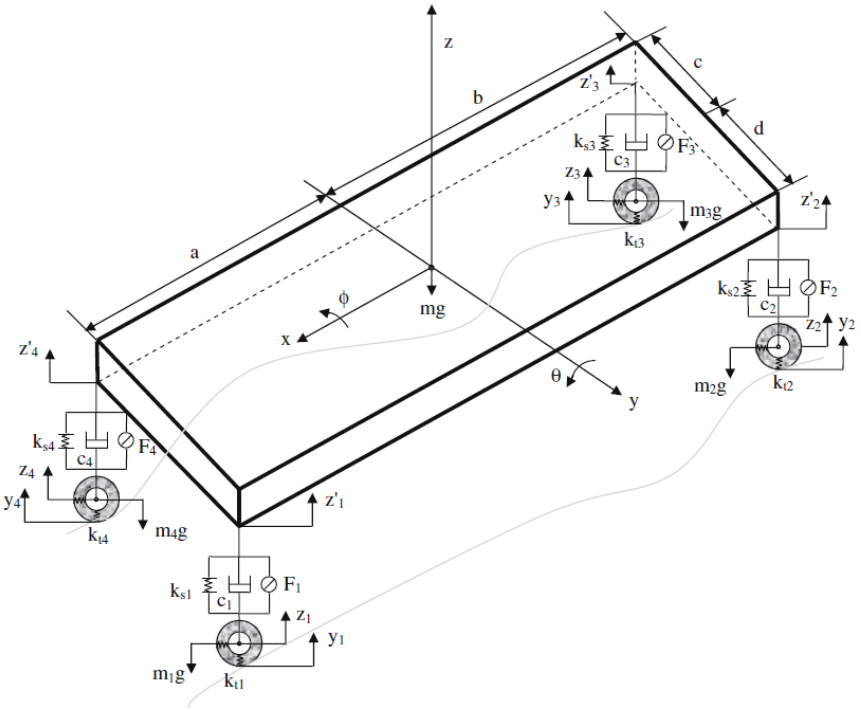

Fig. 1. Complete Vehicle Model

This model incorporates the relative displacement of inelastic masses, including front left suspension mass ($Z_1' - Z_1$), rear left suspension mass ($Z_2' - Z_2$), rear right suspension mass ($Z_3' - Z_3$), right front suspension mass ($Z_4' - Z_4$), and displacement of vertical movement of the vehicle body (Z), along with angular displacements of roll (φ) and pitch (θ) corresponding to the movement of the vehicle body. The specific values for vehicle parameters are outlined in Table 1-2. Through dynamic analysis, the established relationships for the complete vehicle model are as follows:

$$C_{t1}(\dot{z}_1 - \dot{y}_1) = F_{t1} \tag{1}$$

$$C_{t2}(\dot{z}_2 - \dot{y}_2) = F_{t2} \tag{2}$$

$$C_{t3}(\dot{z}_3 - \dot{y}_3) = F_{t3} \tag{3}$$

$$C_{t4}(\dot{z}_4 - \dot{y}_4) = F_{t4} \tag{4}$$

In the above relationships, the parameters C_{t1}, C_{t2}, C_{t3} and C_{t4} represent the damping coefficients of the left front tire, left rear tire, right rear tire and right front tire respectively. Parameters Z_1, Z_2, Z_3 and Z_4 represent the vertical displacement of the front left wheel transmission axis, the vertical displacement of the left rear wheel transmission axis, the vertical displacement of the right rear wheel transmission axis and the vertical displacement of the right front wheel transmission axis of the vehicle respectively. to be The parameters y_1, y_2, y_3 and y_4 respectively indicate the road disturbance input for the left front wheel of the car, the left rear wheel of the car, the right rear wheel of the car and the right front wheel of the car. The parametersF_{t1}, F_{t2}, F_{t3} and F_{t4} represent the force of the front left wheel

of the car, the force of the rear left wheel of the car, the force of the right rear wheel of the car and the force of the front right wheel of the car, respectively.

$$m_1\ddot{z}_1 = k_{t1}(y_1 - z_1) + k_{s1}(\acute{z}_1 - z_1) + c_1\left(\acute{\dot{z}}_1 - \dot{z}_1\right) + F_1 + m_1 g \quad (5)$$

$$m_2\ddot{z}_2 = k_{t2}(y_2 - z_2) + k_{s2}(\acute{z}_2 - z_2) + c_2\left(\acute{\dot{z}}_2 - \dot{z}_2\right) + F_2 + m_2 g \quad (6)$$

$$m_3\ddot{z}_3 = k_{t3}(y_3 - z_3) + k_{s3}(\acute{z}_3 - z_3) + c_3\left(\acute{\dot{z}}_3 - \dot{z}_3\right) + F_3 + m_3 g \quad (7)$$

$$m_4\ddot{z}_4 = k_{t4}(y_4 - z_4) + k_{s4}(\acute{z}_4 - z_4) + c_4\left(\acute{\dot{z}}_4 - \dot{z}_4\right) + F_4 + m_4 g \quad (8)$$

In the above relations, the acceleration of the Earth's gravity is considered equal to g=9.81 m⁄s^2. The parameters m_1, m_2, m_3 and m_4 respectively express the suspension masses of the left front side of the car, the suspension masses of the left rear side of the car, the suspension masses of the right rear side of the car and the suspension masses of the right front side of the car, respectively. Parameters c_1, c_2, c_3 and c_4 respectively represent the damping coefficients of the front left suspension of the car, the suspension of the left rear side of the car, the suspension of the right rear side of the car and the suspension of the right front side of the car. The parameters k_{t1}, k_{t2}, k_{t3} and k_{t4} represent the hardness coefficient of the left front tire, the left rear tire, the right rear tire and the right front tire respectively. The parameters F_1, F_2, F and F_4 respectively indicate the active suspension force on the front left side of the car, the active suspension force on the left rear side of the car, the active suspension force on the right rear side of the car and the active suspension force on the right front side of the car, respectively.

$$m\ddot{z} = k_{s1}(z_1 - \acute{z}_1) + k_{s2}(z_2 - \acute{z}_2) + k_{s3}(z_3 - \acute{z}_3) + k_{s4}(z_4 - \acute{z}_4) + c_1\left(\dot{z}_1 - \acute{\dot{z}}_1\right) + c_2\left(\dot{z}_2 - \acute{\dot{z}}_2\right) + c_3\left(\dot{z}_3 - \acute{\dot{z}}_3\right) + c_4\left(\dot{z}_4 - \acute{\dot{z}}_4\right) - F_1 - F_2 - F_3 - F_4 + mg \quad (9)$$

In the above relationship, m represents the mass of the vehicle body and z shows the displacement of the vehicle body. The parameters k_{s1}, k_{s2}, k_{s3} and k_{s4} respectively indicate the hardness of the front left suspension of the car, the hardness of the rear left suspension, the hardness of the rear right suspension and the hardness of the front right suspension.

$$J_x\ddot{\emptyset} = -\left[k_{s3}(z_3 - \acute{z}_3) + c_3\left(\dot{z}_3 - \acute{\dot{z}}_3\right) + k_{s4}(z_4 - \acute{z}_4) + c_4\left(\dot{z}_4 - \acute{\dot{z}}_4\right)\right]c\left[k_{s1}(z_1 - \acute{z}_1) + c_1\left(\dot{z}_1 - \acute{\dot{z}}_1\right) + k_{s2}(z_2 - \acute{z}_2) + c_2\left(\dot{z}_2 - \acute{\dot{z}}_2\right)\right]d + (F_3 + F_4)c - (F_1 + F_2)d \quad (10)$$

In the above relationship, c represents the distance of the center of gravity from the right transmission axis, d represents the distance from the left transmission axis, J_X represents the moment of inertia of roll and φ also represents the roll angle.

$$J_y\ddot{\theta} = -\left[k_{s1}(z_1 - \acute{z}_1) + c_1\left(\dot{z}_1 - \acute{\dot{z}}_1\right) + k_{s4}(z_4 - \acute{z}_4) + c_4\left(\dot{z}_4 - \acute{\dot{z}}_4\right)\right]a\left[k_{s2}(z_2 - \acute{z}_2) + c_2\left(\dot{z}_2 - \acute{\dot{z}}_2\right) + k_{s3}(z_3 - \acute{z}_3) + c_3\left(\dot{z}_3 - \acute{\dot{z}}_3\right)\right]b + (F_1 + F_4)a - (F_2 + F_3)b \quad (11)$$

In the above relationship, parameter a is equal to the distance of the center of gravity from the front transmission axis of the car, parameter b is equal to the distance of the center of gravity from the rear transmission axis of the car, J_y indicates the amount of pitch moment of inertia and parameter θ also indicates the pitch angle.

$$\acute{z}_1 = z - (a\theta - d\emptyset) \quad (12)$$

$$\acute{z}_2 = z + (b\theta - d\emptyset) \quad (13)$$

$$\acute{z}_3 = z + (b\theta + c\emptyset) \quad (14)$$

$$\acute{z}_4 = z - (a\theta + c\emptyset) \quad (15)$$

The mathematical model of the active suspension is represented by the following state space:

$$\dot{x} = Ax + Bu + d \tag{16}$$

$$y = Cx + Du \tag{17}$$

Where y is the output vector, u is the input vector, A is the state matrix, B is the input matrix, C is the output matrix, D is the feedforward matrix.

3. CONTROL SYSTEMS

To manage the vibration of the full vehicle model, two distinct control structures are employed: the PID controller and the newly devised Robust Neural Network (RNN) control system. The PID controller serves as a baseline for evaluating the performance of the developed RNN control system. The subsequent subsections outline the PID controller and the developed RNN control system. Figure 3.1 illustrates the operational process of the active suspension system for vibration control, depicting the interconnection of various components influencing this process.

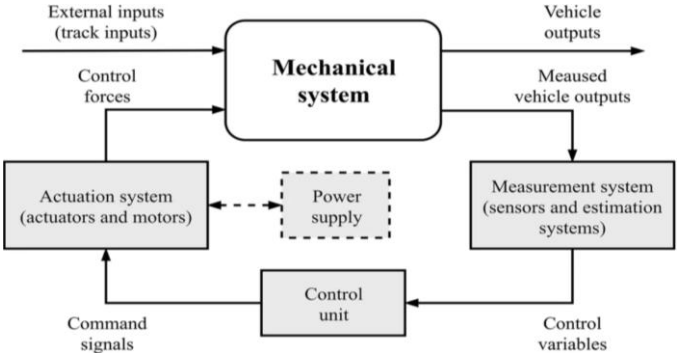

Fig. 2. Workflow of an active suspension [19].

3.1. PID controller

PID controller consists of proportional P(e(t)), integral I(e(t)) and derivative D(e(t)) parts. Assuming that each amplitude is completely decoupled and controlled independently from other amplitudes, the control input F(t) is given by

$$F(t) = K_P e(t) + K_I \int e(t)dt + K_D \frac{de(t)}{dt} \tag{18}$$

In equation, e(t) is the control error;

$$e(t) = x_d(t) - x_a(t) \tag{19}$$

Where $x_d(t)$ is the desired response and $x_a(t)$ is the actual response. K_p is called the proportional gain, K_I the integral gain and K_D the derivative gain. Moreover, Zeigler–Nicholds methods are used to determine the optimum PID gain parameters. Gain parameters of the PID controller.

3.2. Robust neural network (RNN) control system

The proposed control system was designed to control the vehicle system parameters. It consisted of a robust feedback controller and neural network predictive controller. The proposed controller systems' law is given by:

$$F(t) = F_{FB}(t) + F_{NN}(t) \tag{20}$$

Where F_{FB} is the force of robust feedback controller and F_{NN} is the force of the neural network predictive controller.

3.2.1. Robust feedback controller

The PID controller has been widely adopted in the industry due to its simple structure and effectiveness. Despite its prevalence, the conventional PID controller's constant gain parameters may not be optimal for reducing velocity control errors. To address this limitation, an exponential function is introduced to the derivative component of the conventional PID controller. This addition facilitates an exponential decrease of the error term (*e(t)*). In this application, a robust feedback controller architecture is proposed, with the initial segment of the control input described as follows:

$$F_{FB}(t) = K_P e(t) + K_I \int e(t)dt + K_D \frac{de(t)}{dt} (K_R(e^{(-K_{R1}t)}) \quad (21)$$

where K_P ،K_D ،K_I ،K_R and K_{R1} are the robust controller part gain matrices. $(K_R e^{(-K_{R1}t)})$ parameters are developed to control vibration parameters of the vehicle's suspension for different road roughness. Method of trial and error is used to determine the $\left(K_R e^{(-K_{R1}t)}\right)$ parameters of robust controller. The parameters of the controller were set by empirically after long training.

3.2.2. Neural network control system

In this section, we introduce the mobile form system model and illustrate how this model can be effectively identified using a neural network. Subsequently, we elaborate on the utilization of the identified neural network model as a controller.

Reference model control minimizes the need for extensive online calculations. However, unlike the preceding controller, the reference model controller necessitates an offline-trained neural network. The computational expense associated with training this network is relatively high, as it employs the error backpropagation algorithm. The notable advantage of employing this network lies in its versatility, allowing its application to systems with greater diversity compared to the previous controller.

4. LUNBERG-MARQUARDT ALGORITHM (LMA)

The backpropagation algorithm, while widely used, has inherent drawbacks such as slow convergence speed and the tendency to settle at local minimum points before the neural network completes learning. To address these issues, we have opted to enhance the training process by employing a feed-forward neural network trained with the Lönberg-Marquardt algorithm. Unlike the constant learning rate in backpropagation, the Lönberg-Marquardt algorithm adjusts the learning rate dynamically during training.

Among various error backpropagation-based training methods, we have selected the Lönberg-Marquardt algorithm for its faster convergence in training medium-sized networks. This algorithm alters the network weights and bias values in a manner that minimizes the performance function more rapidly. Essentially, the Lönberg-Marquardt algorithm is a technique for minimizing a multivariable nonlinear function, widely used for solving the least squares problem associated with nonlinear functions.

The Lönberg-Marquardt algorithm combines aspects of the Gauss-Newton algorithm and the gradient descent method, providing more consistency than the Gauss-Newton algorithm. It interpolates between these methods, making it robust and capable of finding solutions even when starting far from the final minimum. While slightly slower than the Gauss-Newton algorithm for well-behaved functions and reasonable initial parameters, the Lönberg-Marquardt algorithm stands out as the most popular curve-fitting algorithm.

This algorithm effectively adjusts the weights of a neural network from random initial conditions. When the neural network's initial weights are randomly set, the Lönberg-Marquardt algorithm serves to fine-tune these weights. Similar to Newton's pseudo-methods, the Lönberg-Marquardt algorithm is designed to achieve efficient second-order neural network training without the need to compute the Hessian matrix. When the performance

function takes the form of the sum of squares, as is common in neural networks, the Hessian matrix can be approximated as follows:

$$H = J^T J \tag{22}$$

Its gradient can also be calculated as follows:

$$grad = J^T\, e(t) \tag{23}$$

In this algorithm, the following approximation is used to calculate the Hessian matrix, and the weight correction value is calculated as follows:

$$\Delta W = -[J^T J + \mu I]^{-1} J^T e(t) \tag{24}$$

An advantageous aspect of the Lönberg-Marquardt algorithm is its adaptability, demonstrated by its behavior depending on the value of μ. As μ increases, the algorithm approaches the maximum gradient descent algorithm with a low training rate, resembling Gauss-Newton when μ is very small. In the provided relationship, the J matrix signifies the Jacobian matrix, encompassing the first derivatives of neural network errors concerning its weights and bias values. Additionally, the parameter e(t) denotes the network errors. Calculating the Jacobian matrix can be achieved through the standard error backpropagation method, which boasts significantly lower computational complexity compared to Hessian matrix calculations.

5. SIMULATION RESULTS AND DISCUSSION

In this section, we conduct simulations of the active suspension system for the specified modes and subsequently compare the obtained simulation results. This process involves six transformation functions, each connected to a reference model. Multiple reference models are considered for this process. The desired process, namely the suspension system, is then examined in distinct segments, including:

1. The relative displacement of the active suspension system on the left side of the front of the vehicle $(Z_1' - Z_1)$
2. The relative displacement of the active suspension system on the rear left side of the vehicle $(Z_2' - Z_2)$
3. The relative displacement of the active suspension system on the right rear side of the vehicle $(Z_3' - Z_3)$
4. The relative displacement of the active suspension system on the right front of the vehicle $(Z_4' - Z_4)$

Certainly, let's discuss the results of the simulation in the two cases: without a controller and with a robust neural network control system.

5.1. Without a Controller

Roll Angle Response (φ): The simulation shows the behavior of the active car suspension system in response to the angular displacement caused by the random road profile. Without a controller, the system relies solely on the inherent characteristics of the suspension, leading to uncontrolled oscillations or movements in the roll angle.

Pitch Angle Response (θ): Similarly, the simulation illustrates the system's response to the angular displacement of the vehicle's pitch due to the random road profile. Without active control, the pitch angle might exhibit unregulated variations, impacting the stability and comfort of the vehicle.

5.2. With Robust Neural Network Control System

Roll Angle Response (φ): In this case, the robust neural network control system actively manages and adjusts the suspension in response to the random road profile. The system aims to minimize deviations in the roll angle, providing a more stable and controlled behavior compared to the uncontrolled scenario.

Pitch Angle Response (θ): The robust neural network control system intervenes to optimize the pitch angle response, ensuring a smoother and controlled movement of the vehicle in reaction to the irregularities in the road profile. This contributes to enhanced stability and comfort.

In summary, the comparison highlights the effectiveness of the robust neural network control system in mitigating undesirable effects, offering better control over the vehicle's roll and pitch angles in response to random road irregularities.

5.3. Active suspension without the use of a controller

The block diagram of the active suspension without the use of a controller is shown in Figure 5.1.

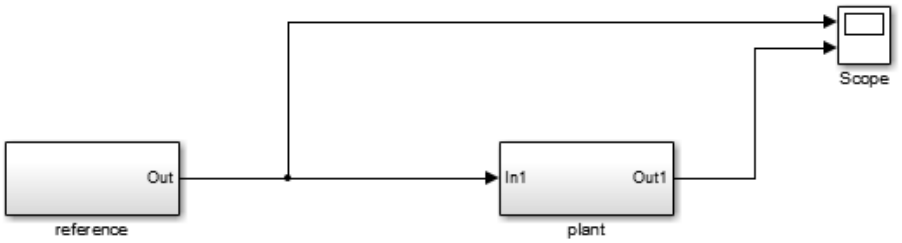

Fig. 3. Block diagram of the suspension system without a controller.

The six conversion functions considered in the process block are as follows.

$$Z_1' - Z_1 = \frac{1}{s+1}$$

$$Z_2' - Z_2 = \frac{s+999}{s^2+1001s+1000}$$

$$Z_3' - Z_3 = \frac{s^3+49s^2+698s+3080}{s^4+52s^3+789s^2+3978s+3240}$$

$$Z_4' - Z_4 = \frac{1.3s^3+68.9s^2+6851s+1866}{s^4+50.5s^3+551s^2+1945s+1443}$$

$$\emptyset = \frac{s^2+21s+101}{s^3+22.3s^2+134.2s+112.9}$$

$$\theta = \frac{s^2+21s+110}{s^3+22s^2+129s+108}$$

The block diagram of the vehicle's active suspension system without the use of a controller is as follows.

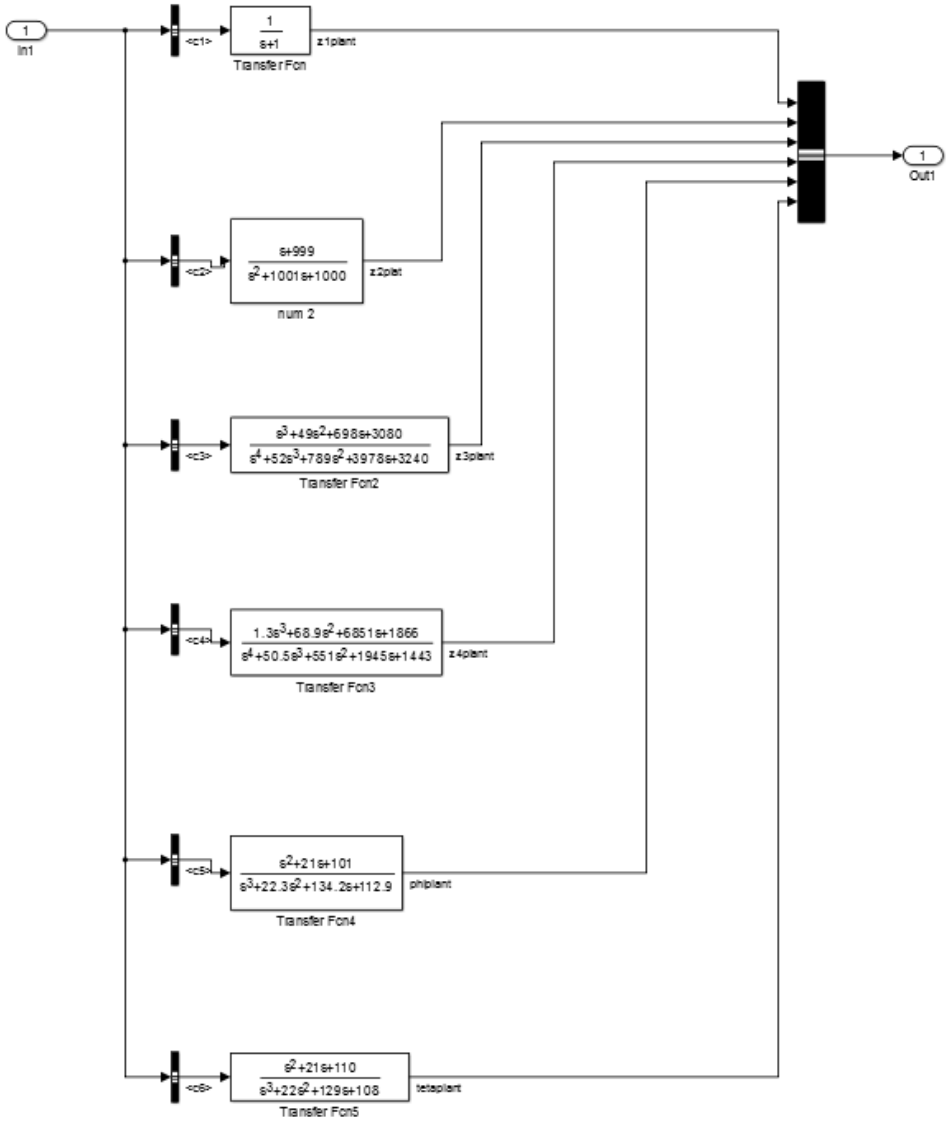

Fig. 4. Block diagram of the six investigated modes of the vehicle suspension system

Also, several different reference entries are used in the reference block:

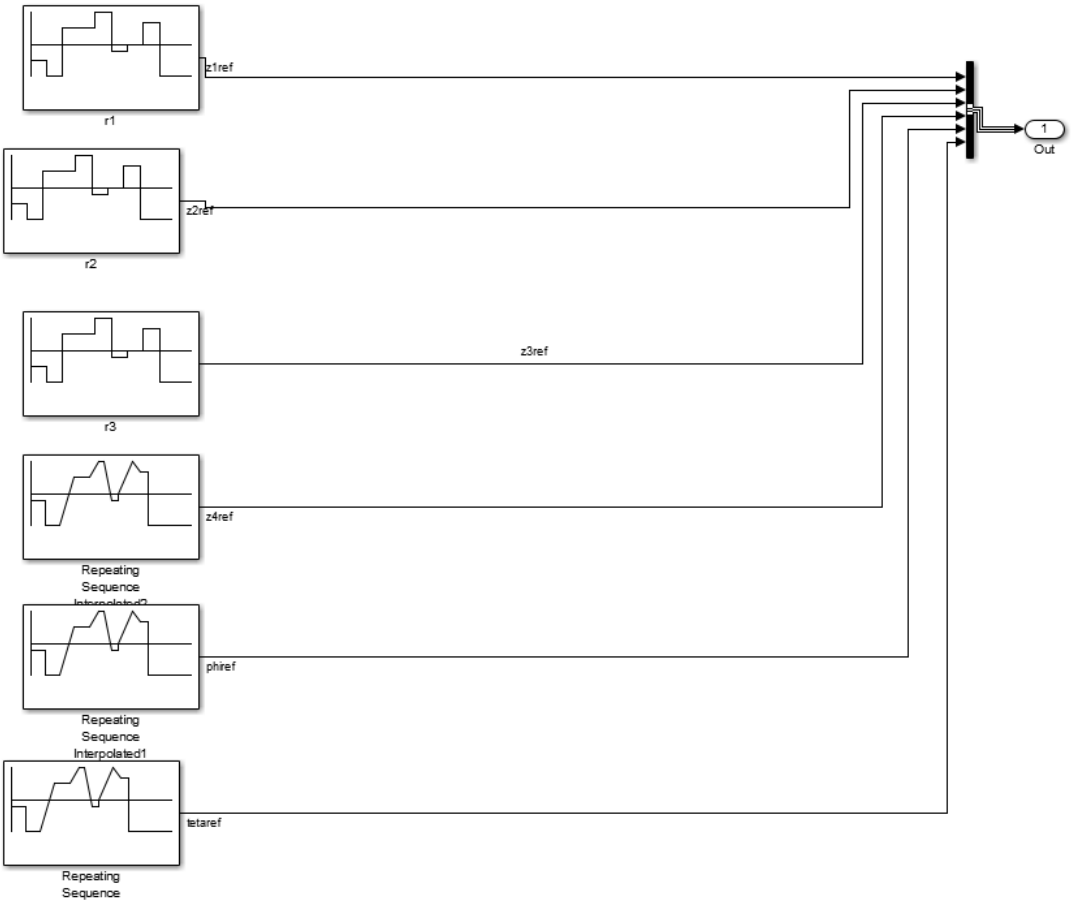

Fig. 5. Reference model of vehicle active suspension system

The simulation response of the vehicle's active suspension system against the profile of random road irregularities without the use of a controller can be seen in the following figures.

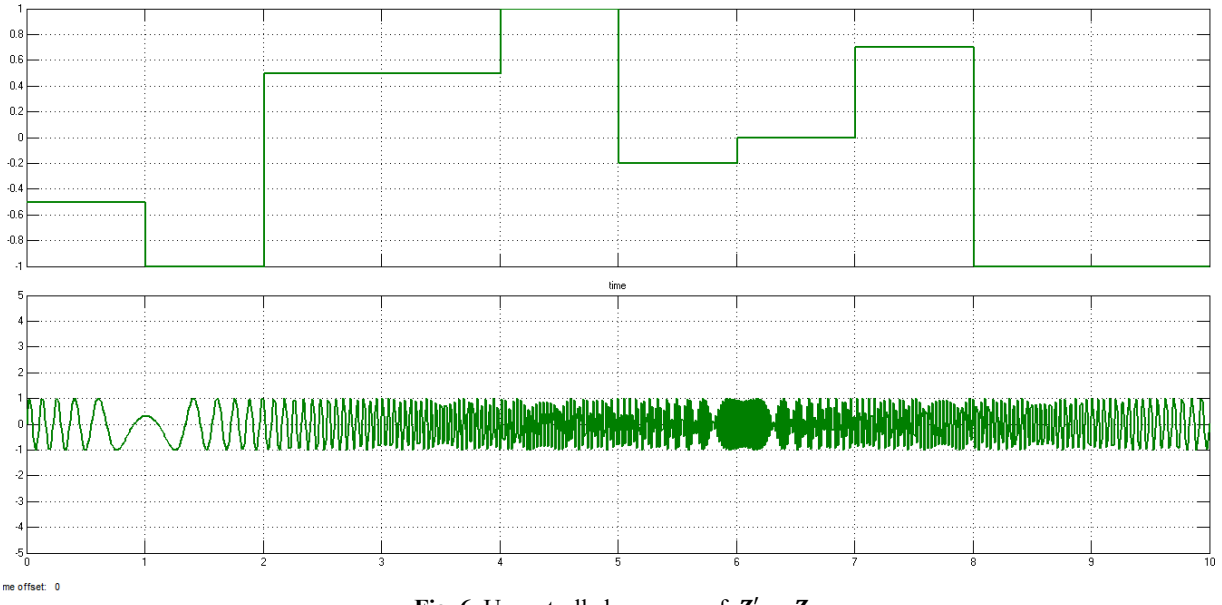

Fig. 6. Uncontrolled response of $Z_1' - Z_1$

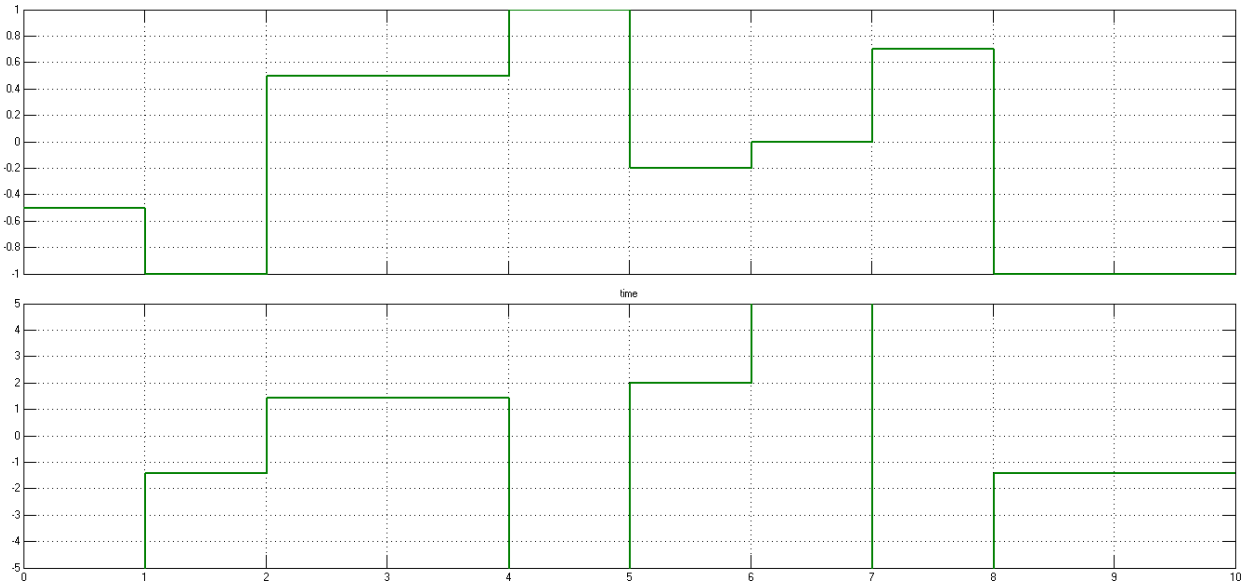

Fig. 7. Uncontrolled response of $Z_2' - Z_2$

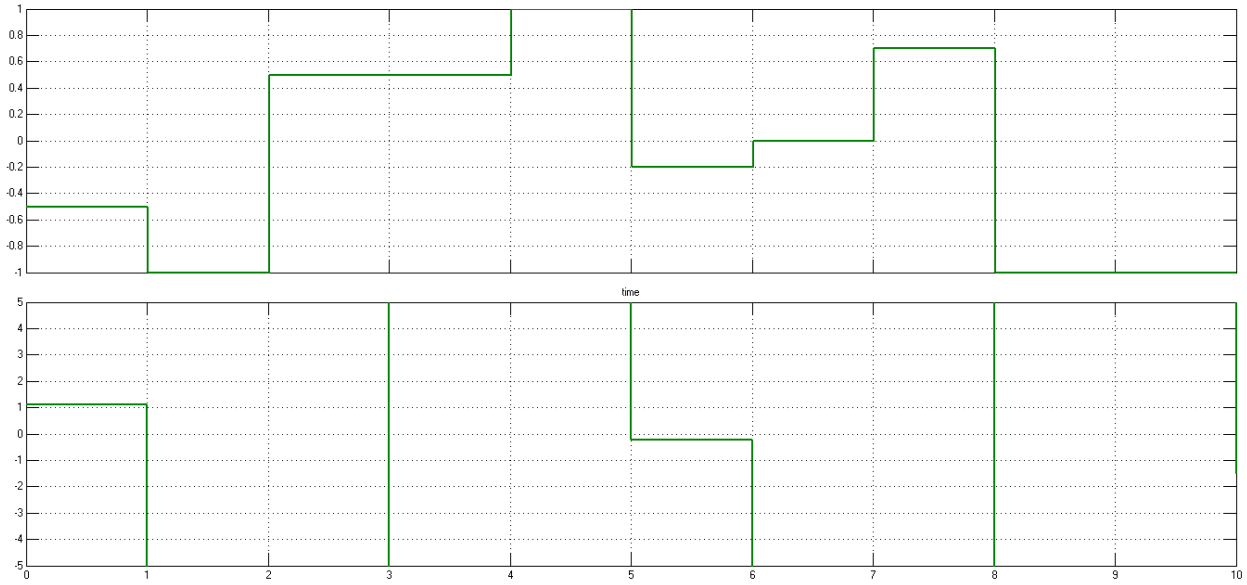

Fig. 8. Uncontrolled response of $Z_3' - Z_3$

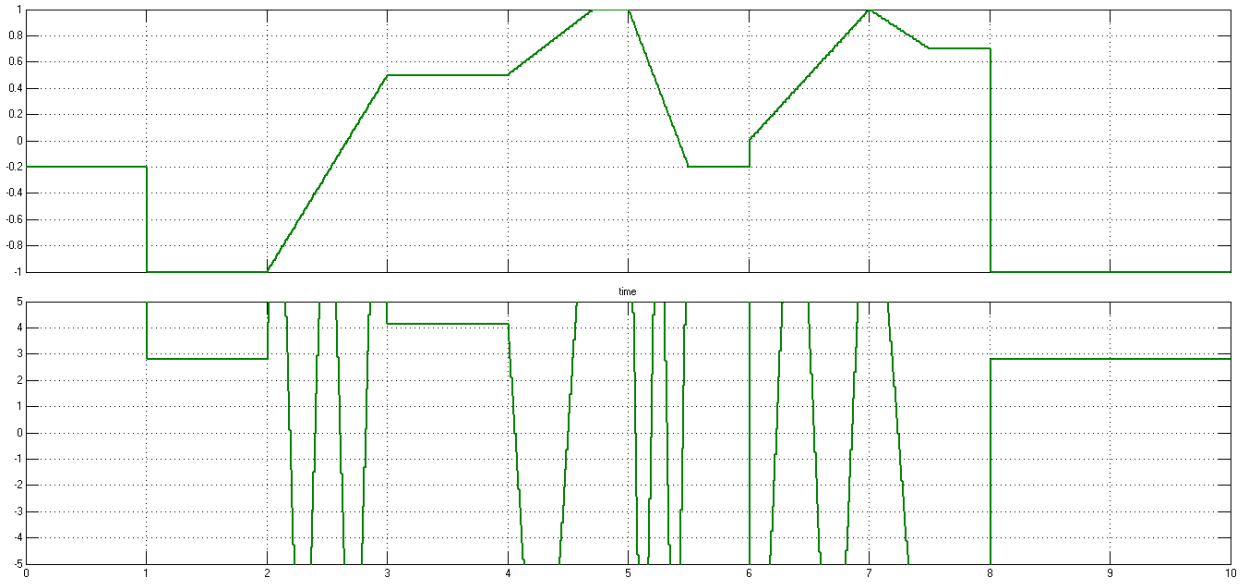

Fig. 9. Uncontrolled response of $\mathbf{Z_4' - Z_4}$

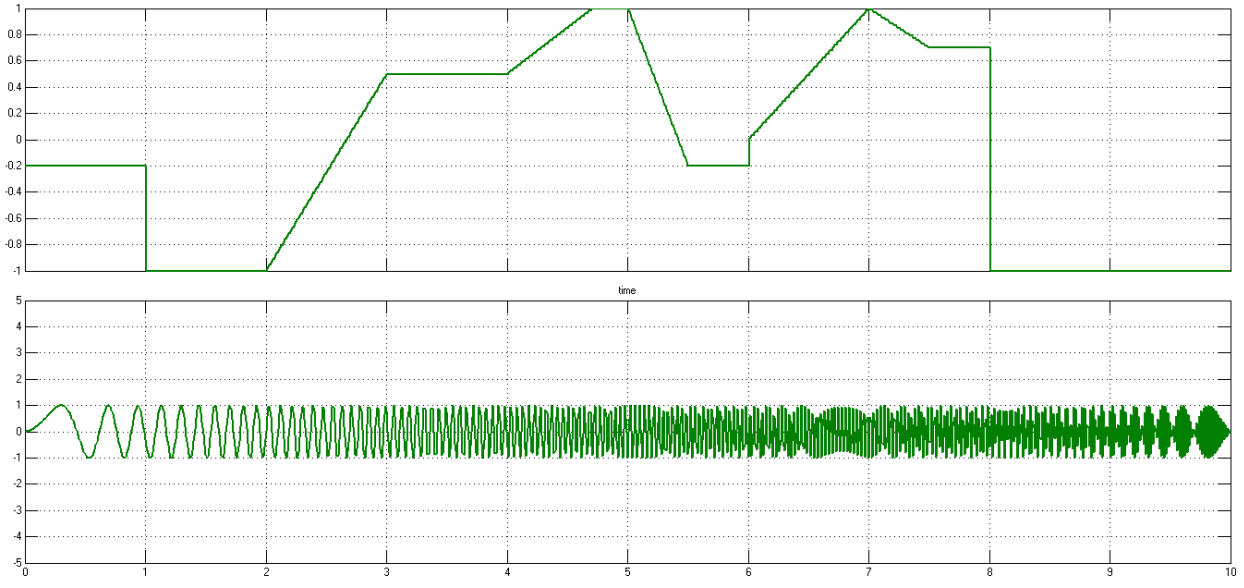

Fig. 10. Uncontrolled response of $\boldsymbol{\varphi}$

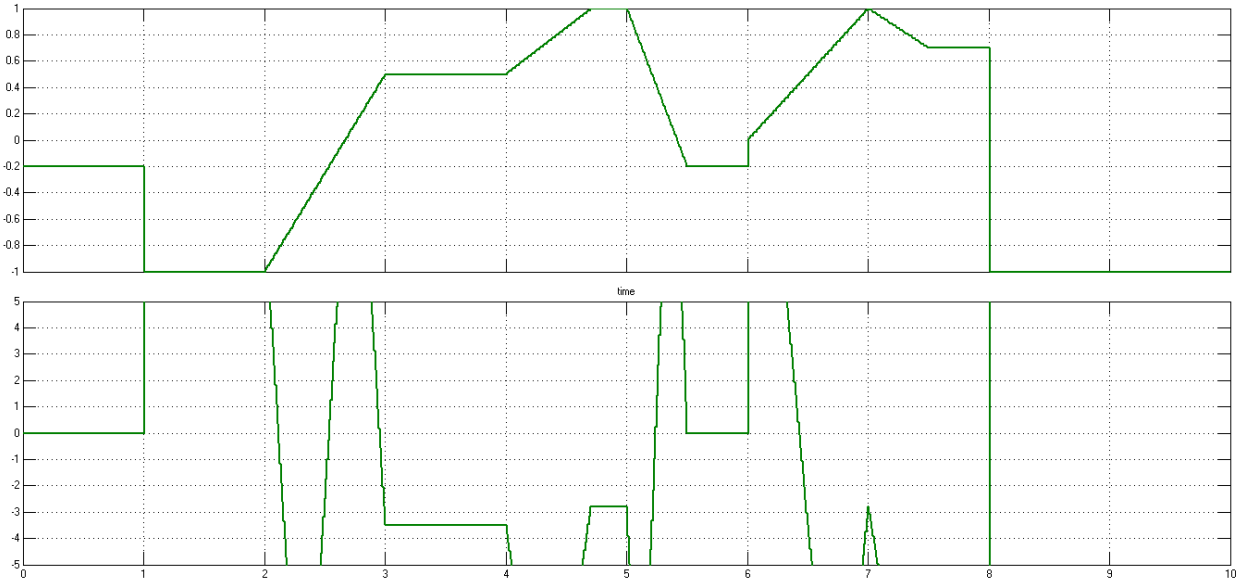

Fig. 11. Uncontrolled response of **θ**

According to the results of the simulation of the active vehicle suspension system without using a controller, which shows the response of the active vehicle suspension system to the profile of random road irregularities without using any kind of controller, it can be concluded that The uncontrolled response does not track the amount of random road roughness profile and has the largest amount of error between the reference input and the output.

Therefore, in order to have the desired tracking, it is necessary to use a controller to reduce the approximation error. In the following, two integral proportional controllers and a robust neural network have been used. By comparing their answers, the better performance of each can be estimated.

5.4. Control of active vehicle suspension system using robust neural network (RNN) controller

Now we simulate the desired process for the mode described in the previous section, using a robust neural network controller, and examine the response of each of them. The block diagram of the vehicle suspension system using the robust neural network control system is shown in Figure.

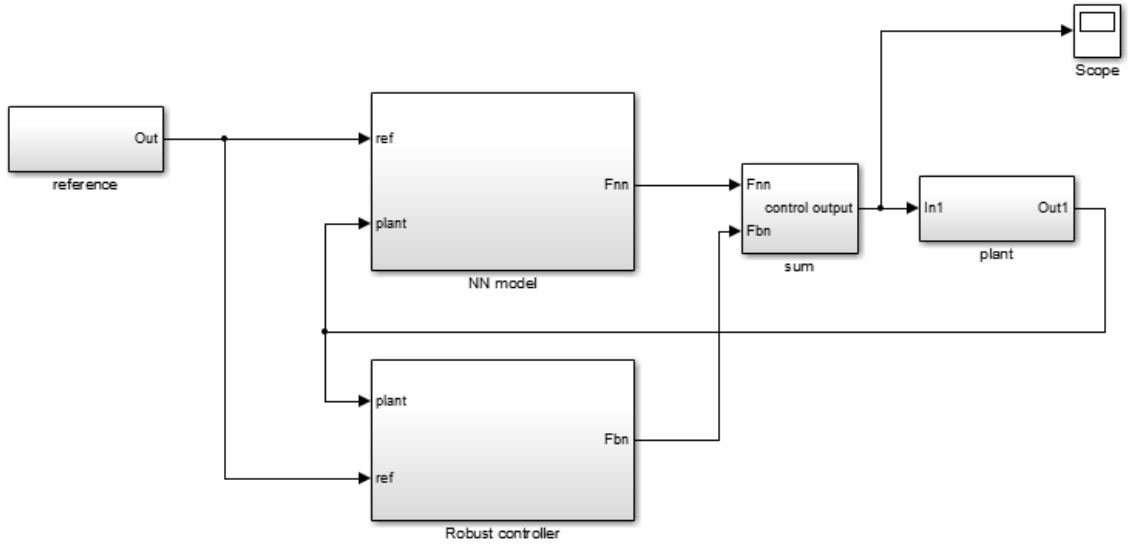

Fig. 12. Block diagram of the suspension system using a robust neural network control system.

The block diagram of each sub-system which is controlled by using the robust neural controller can be seen below.

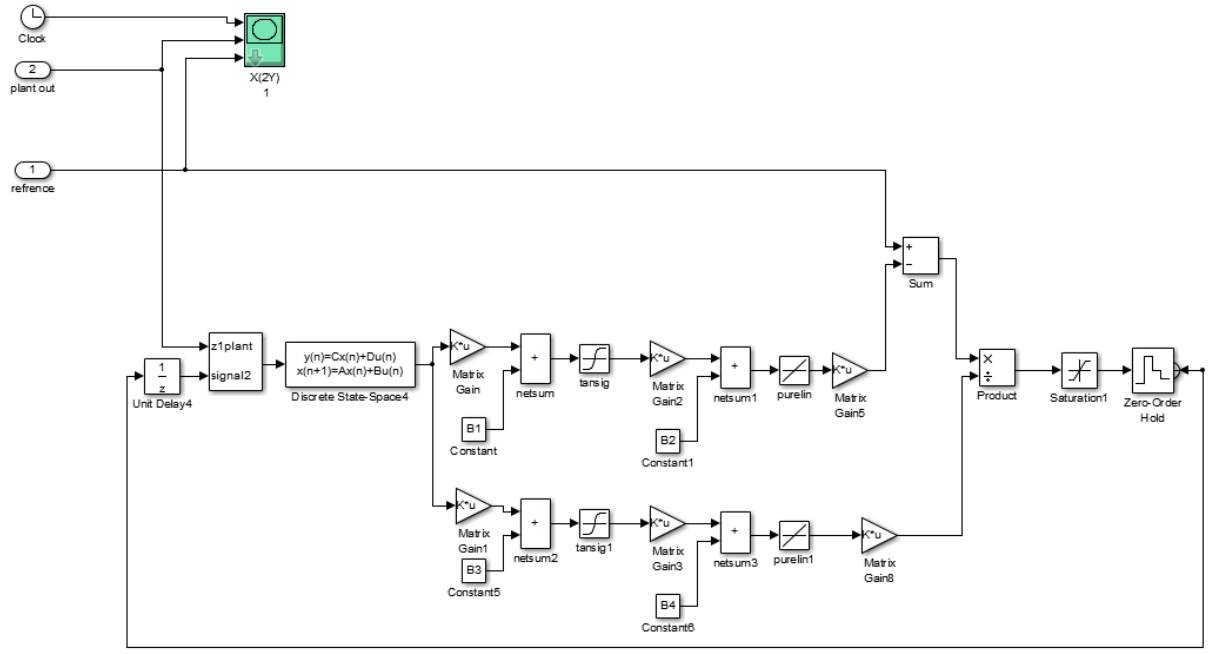

Fig. 14. Controlled response of $\mathbf{Z_1' - Z_1}$ function using a robust neural network control system.

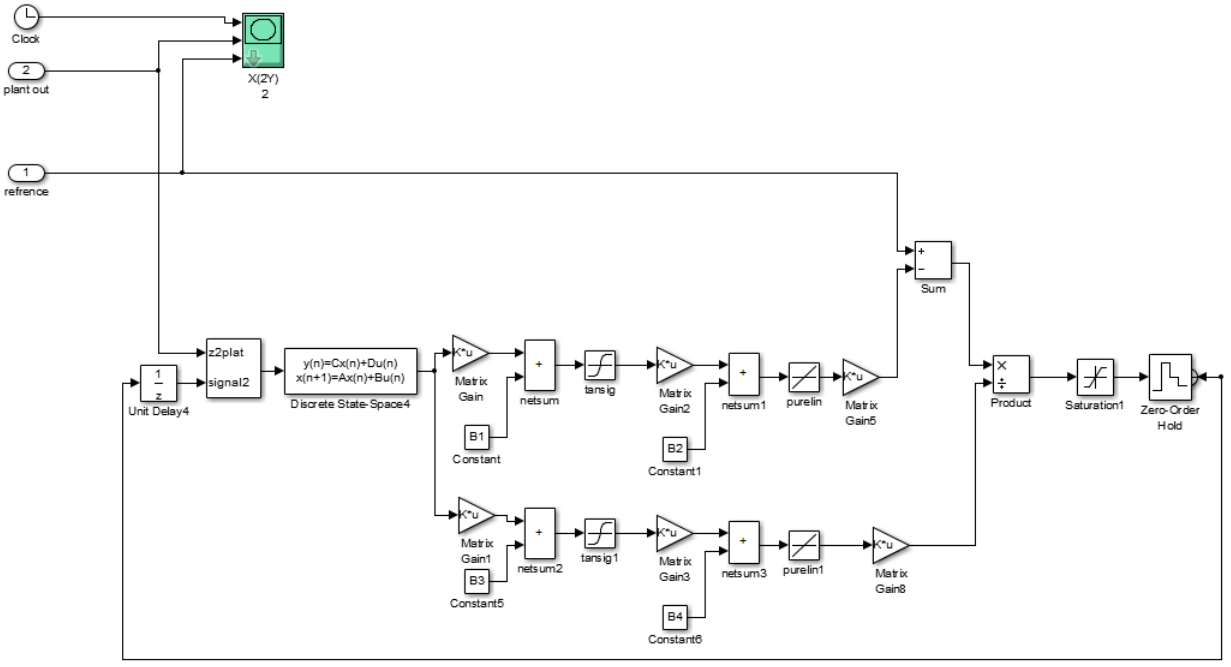

Fig. 15. Controlled response $\mathbf{Z_2' - Z_2}$ function using a robust neural network control system.

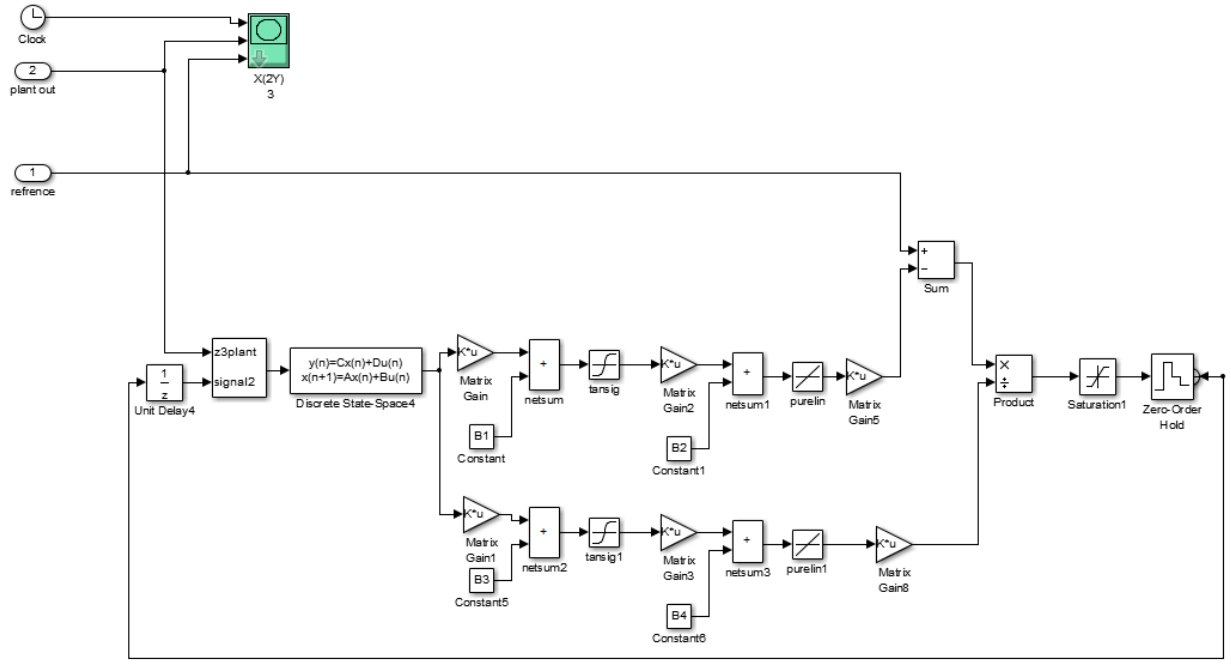

Fig. 16. Controlled response $\mathbf{Z_3'} - \mathbf{Z_3}$ function using a robust neural network control system.

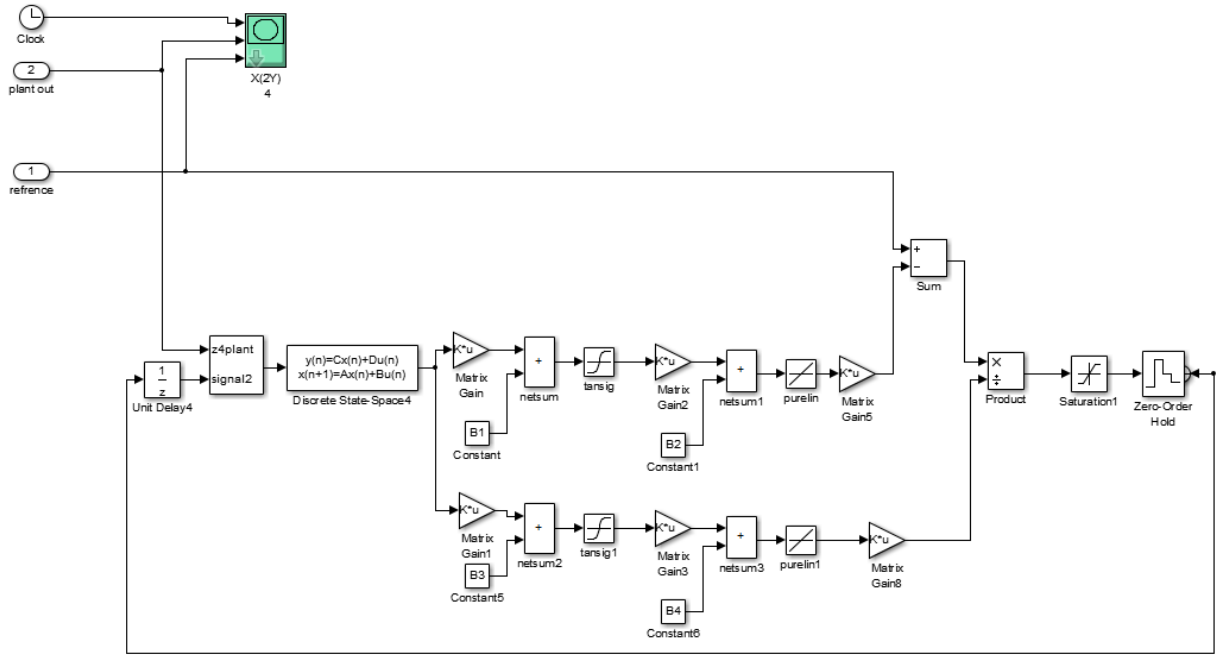

Fig. 17. Controlled response $\mathbf{Z_4'} - \mathbf{Z_4}$ function using a robust neural network control system.

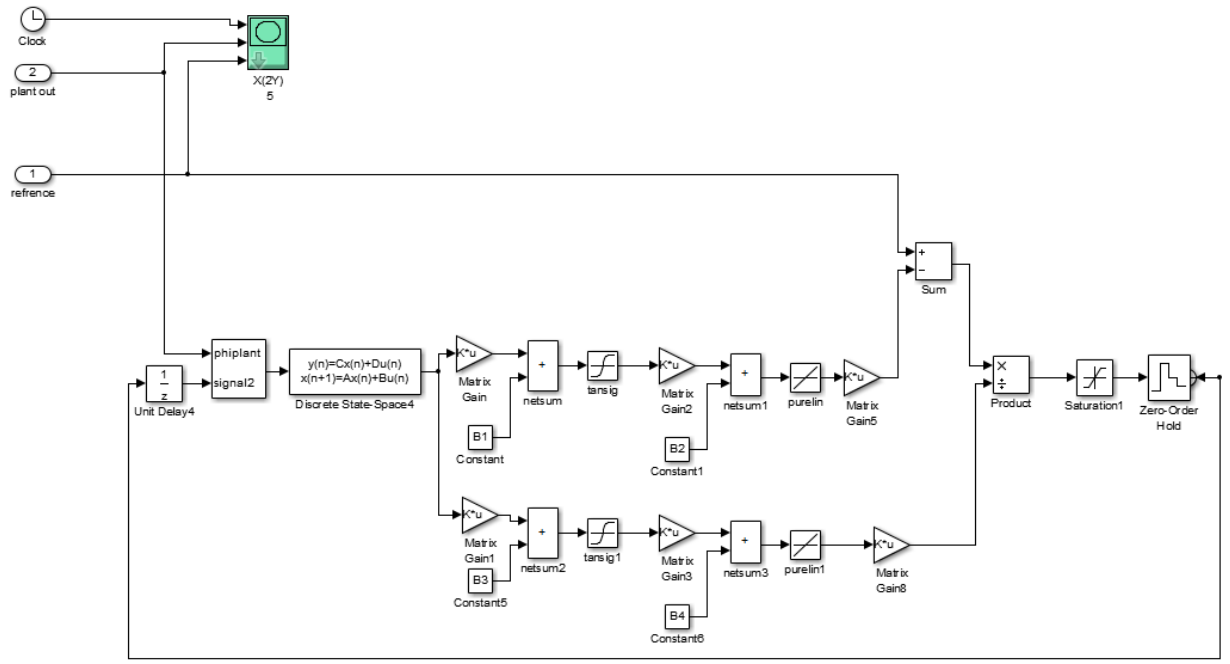

Fig. 18. Controlled response **φ** function using a robust neural network control system.

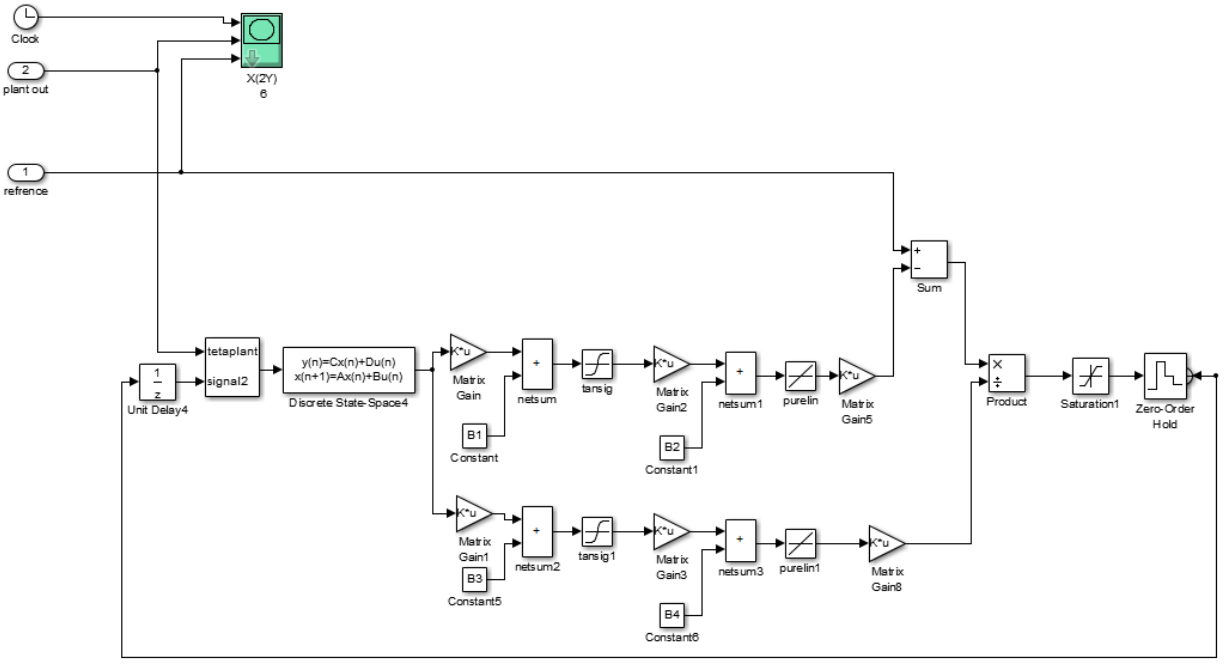

Fig. 19. Controlled response **θ** function using a robust neural network control system.

It should be noted that due to the use of the post-propagation algorithm in the designed neural network, continuous and differentiable activation functions should be used as the activation functions of the hidden layers and the output of the neural network. Because in the post-propagation calculations in the post-propagation algorithm, it is necessary to calculate the derivative of the activation function, and if we consider the activation function discretely, we are not able to calculate its derivative and we cannot use the post-propagation algorithm Let's implement. Therefore, hyperbolic logarithm (logsig), hyperbolic tangent (tansig) and linear function (purelin) functions can be used as activation functions of hidden and output layers in the designed neural network. Below, several different modes of

using these functions as neural network activation functions are simulated and their results are compared with each other.

At first, we consider the activation functions of the hidden layer as a non-linear function of the hyperbolic logarithm (logsig) and the activation function of the output layer as a linear function (purelin). The simulation results of the control of the vehicle's active suspension system against the accidental road unevenness profile using the resilient neural network control system can be seen in the figures below.

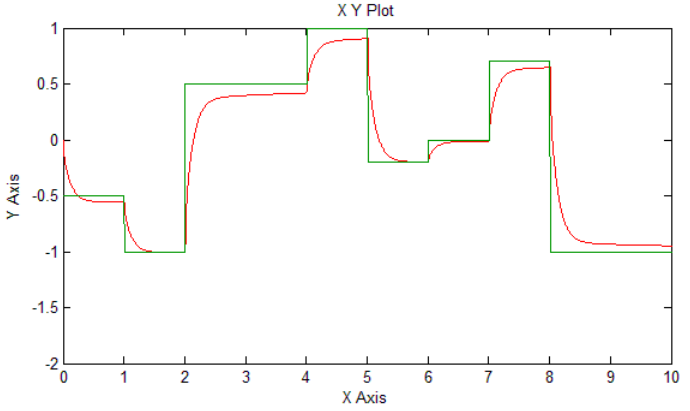

Fig. 20. Controlled response of $\mathbf{Z_1' - Z_1}$ using the hyperbolic logarithm activation function in the hidden layer of the robust neural network controller.

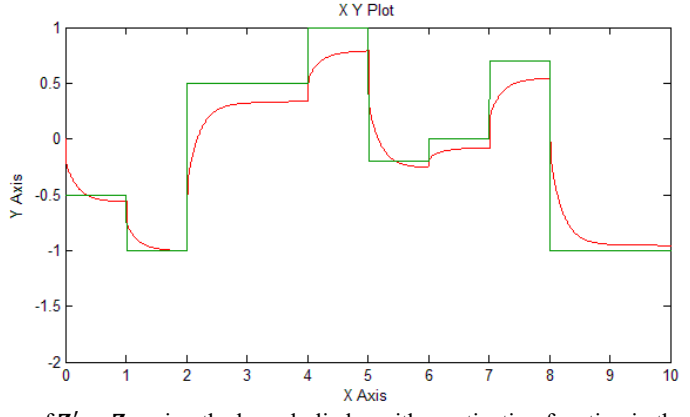

Fig. 21. Controlled response of $\mathbf{Z_2' - Z_2}$ using the hyperbolic logarithm activation function in the hidden layer of the robust neural network controller

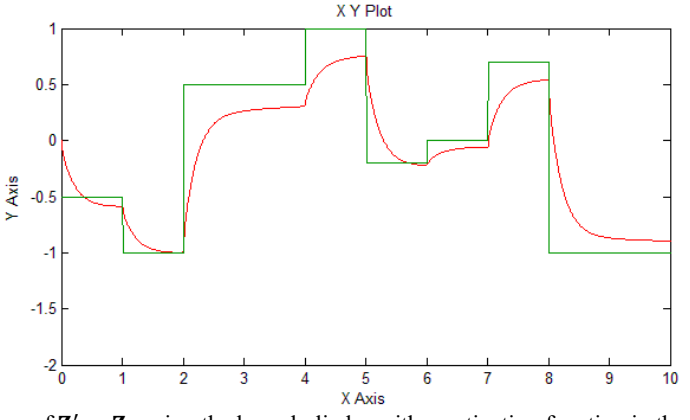

Fig. 22. Controlled response of $\mathbf{Z_3' - Z_3}$ using the hyperbolic logarithm activation function in the hidden layer of the robust

neural network controller

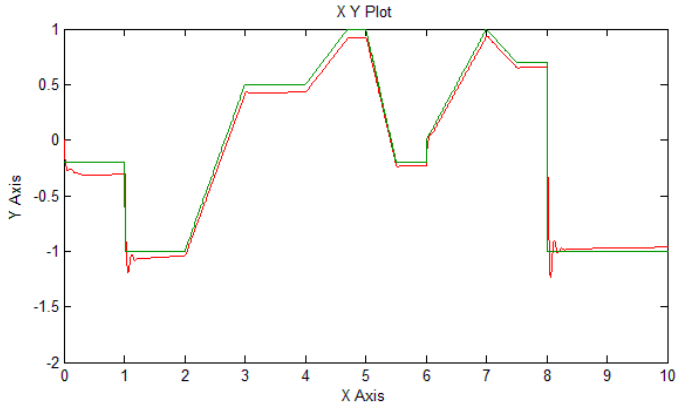

Fig. 23. Controlled response of $\mathbf{Z_4' - Z_4}$ using the hyperbolic logarithm activation function in the hidden layer of the robust neural network controller

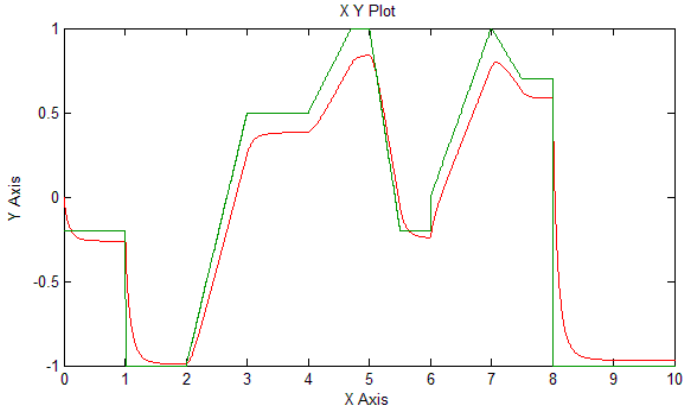

Fig. 24. Controlled response of $\boldsymbol{\varphi}$ using the hyperbolic logarithm activation function in the hidden layer of the robust neural network controller

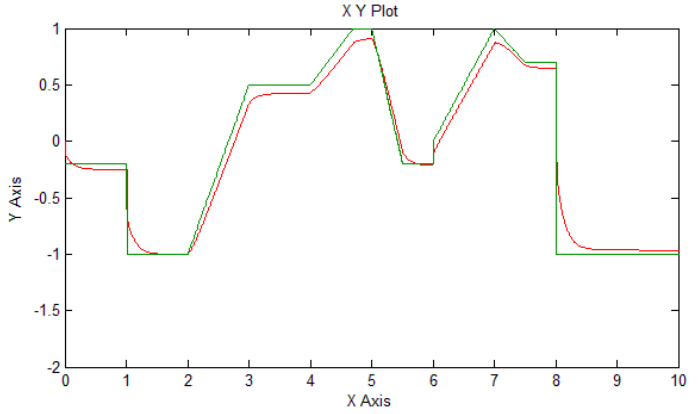

Fig. 25. Controlled response of $\boldsymbol{\theta}$ using the hyperbolic logarithm activation function in the hidden layer of the robust neural network controller

Now we consider the activation functions of the hidden layer as a non-linear hyperbolic tangent function (tansig) and the activation function of the output layer as a linear function (purelin). The simulation results of the control of

the vehicle's active suspension system against random road unevenness profiles using the robust neural network control system can be seen in the following figures.

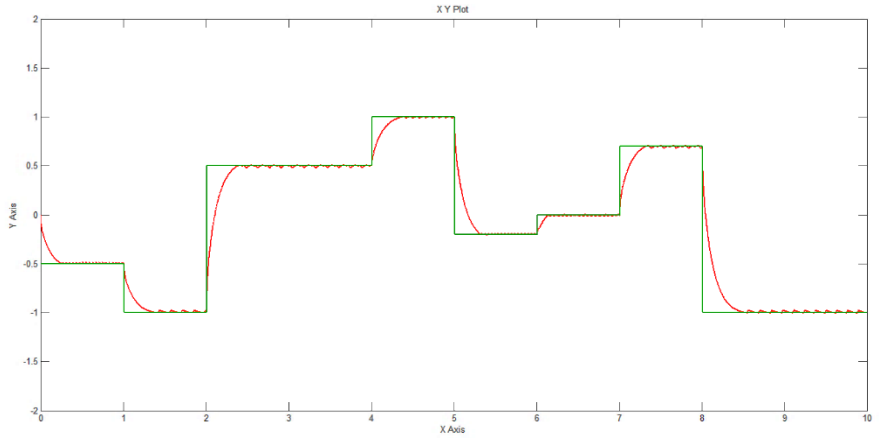

Fig. 26. Controlled response of $\mathbf{Z_1' - Z_1}$ using the hyperbolic tangent activation function in the hidden layer of the robust neural network controller.

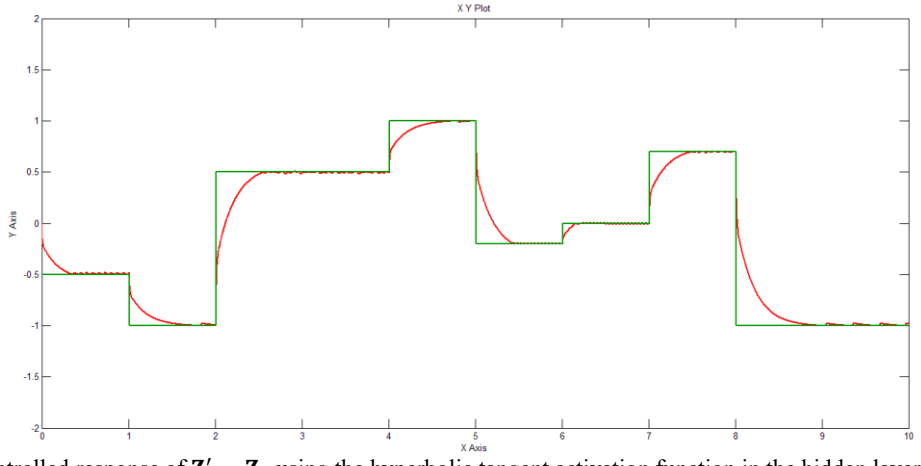

Fig. 27. Controlled response of $\mathbf{Z_2' - Z_2}$ using the hyperbolic tangent activation function in the hidden layer of the robust neural network controller

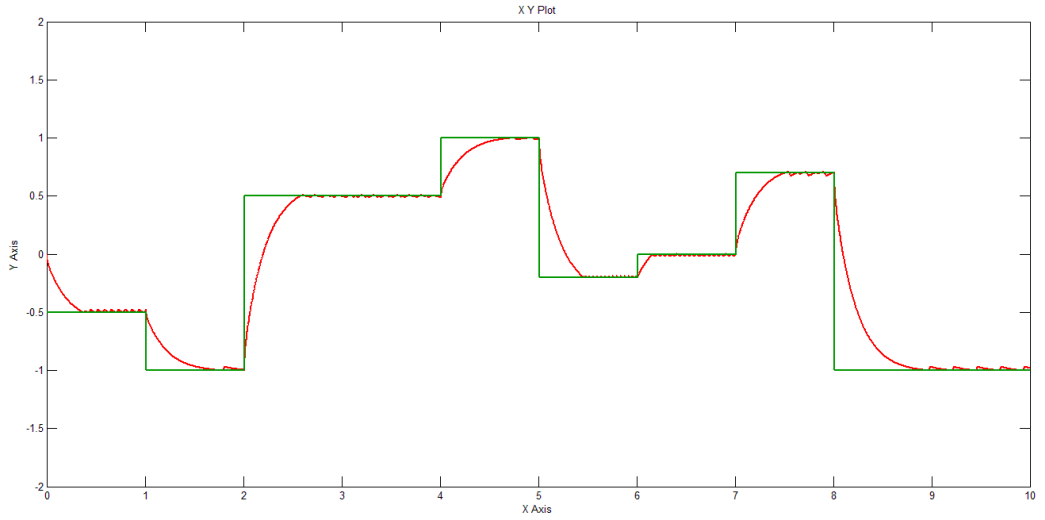

Fig. 28. Controlled response of $\mathbf{Z_3' - Z_3}$ using the hyperbolic tangent activation function in the hidden layer of the robust neural network controller

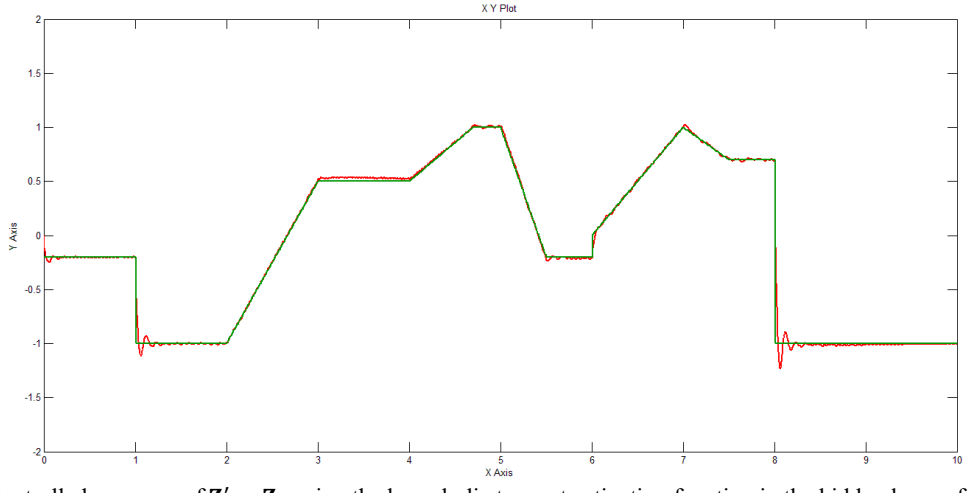

Fig. 29. Controlled response of $\mathbf{Z_4' - Z_4}$ using the hyperbolic tangent activation function in the hidden layer of the robust neural network controller

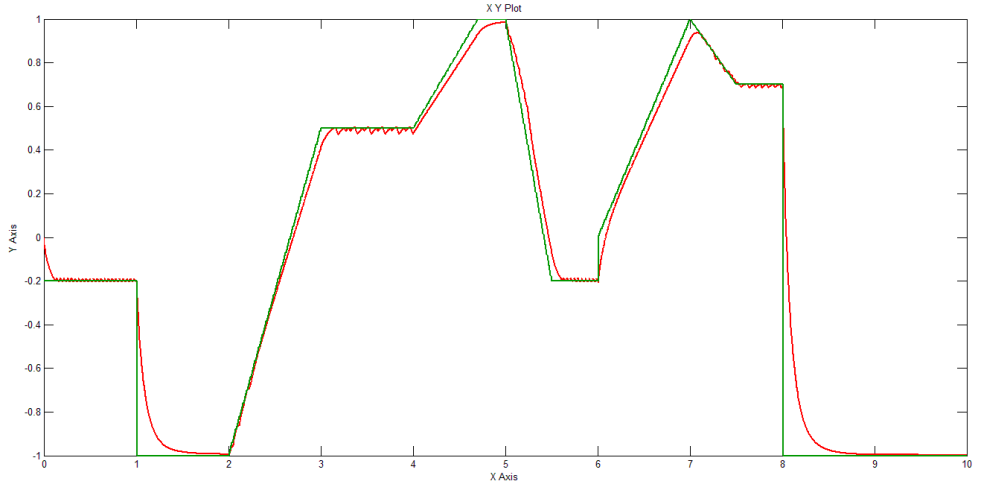

Fig. 30. Controlled response of **φ** using the hyperbolic tangent activation function in the hidden layer of the robust neural network controller

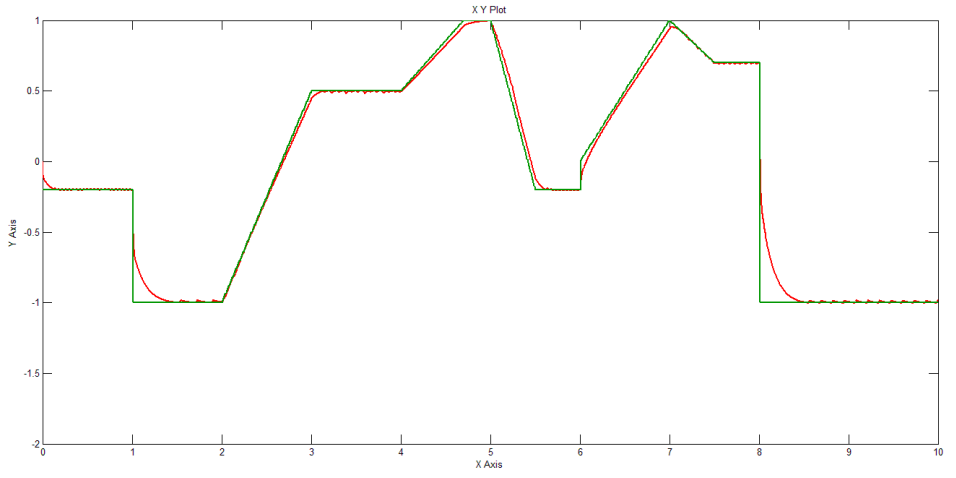

:

Fig. 31. Controlled response of **θ** using the hyperbolic tangent activation function in the hidden layer of the robust neural network controller

By comparing the controlled responses of the functions $Z_1' - Z_1, Z_2' - Z_2, Z_3' - Z_3, Z_4' - Z_4$, φ and θ in two cases, i.e. using nonlinear activation functions of hyperbolic tangent and hyperbolic logarithms in the hidden layer, it can be seen that the tracking error of the reference input in the first case, where the hyperbolic logarithm function was used as the activation function in the hidden layer, compared to the approximation error by the neural network in the second case, which was the tangent function The hyperbola was used as the activation function in the hidden layer. In other words, for better approximation by the neural network and to reduce the tracking error of the control reference, it is recommended to use the hyperbolic tangent nonlinear function as the activation function in the hidden layer. Also, in general, the resilient neural network control system has well controlled the active suspension system of the vehicle against the accidental road irregularities and has performed the desired tracking action between the reference input and the output with a very small amount of error. Therefore, the robust neural network controller can be used to control the active suspension system of the vehicle to have a more suitable performance and a very low and close to zero error.

In order to compare the effect of the activation function in the output layer of the neural network, the activation functions of the hidden and output layers can be considered as a non-linear hyperbolic tangent function (tansig). The simulation results of the control of the vehicle's active suspension system against random road unevenness profiles using the robust neural network control system can be seen in the following figures.

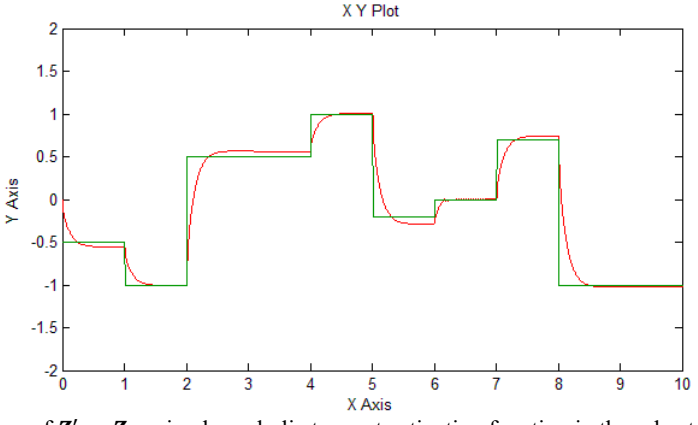

Fig. 32. Controlled response of $\boldsymbol{Z_1' - Z_1}$ using hyperbolic tangent activation function in the robust neural network controller

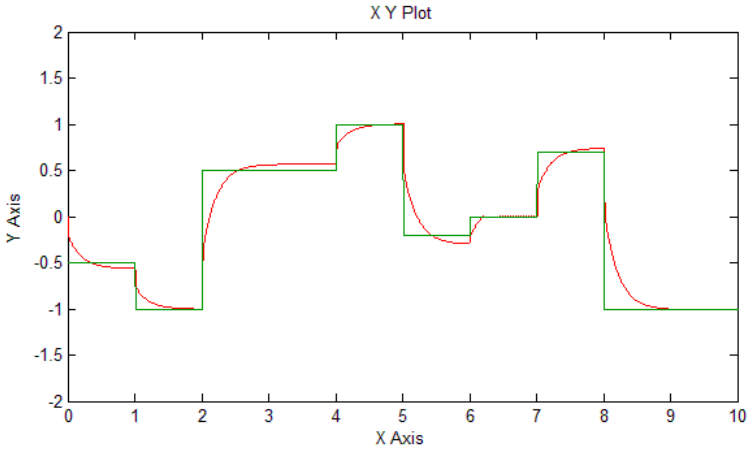

Fig. 33. Controlled response of $Z_2' - Z_2$ using hyperbolic tangent activation function in the robust neural network controller

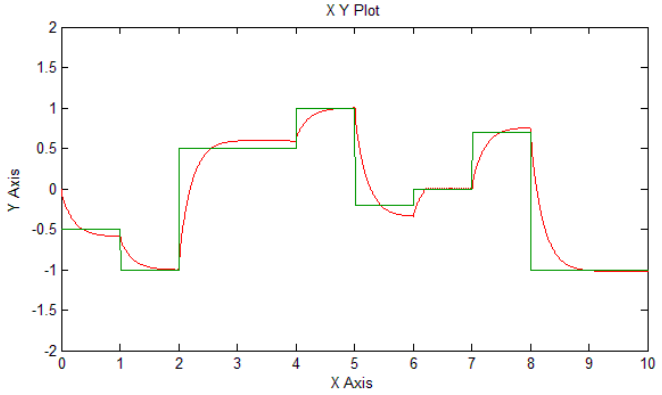

Fig. 34. Controlled response of $Z_3' - Z_3$ using hyperbolic tangent activation function in the robust neural network controller

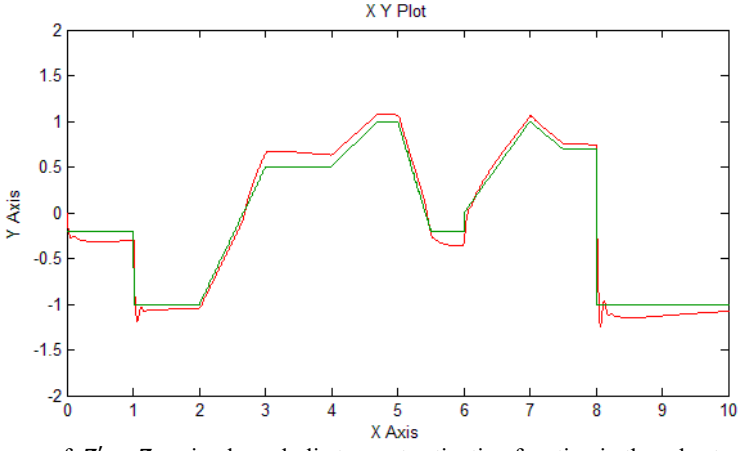

Fig. 35. Controlled response of $Z_4' - Z_4$ using hyperbolic tangent activation function in the robust neural network controller

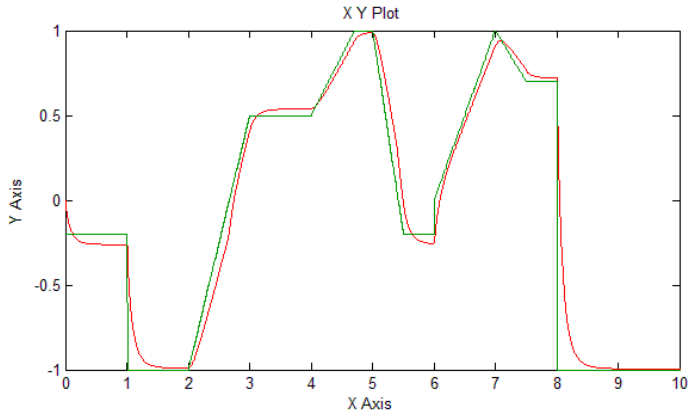

Fig. 36. Controlled response of $\boldsymbol{\varphi}$ using hyperbolic tangent activation function in the robust neural network controller

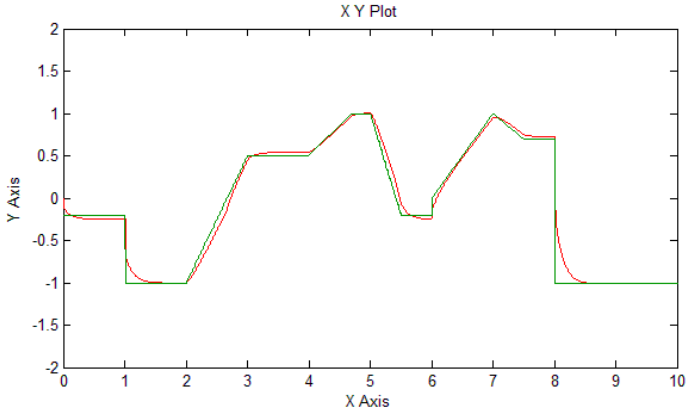

Fig. 37. Controlled response of $\boldsymbol{\theta}$ using hyperbolic tangent activation function in the robust neural network controller

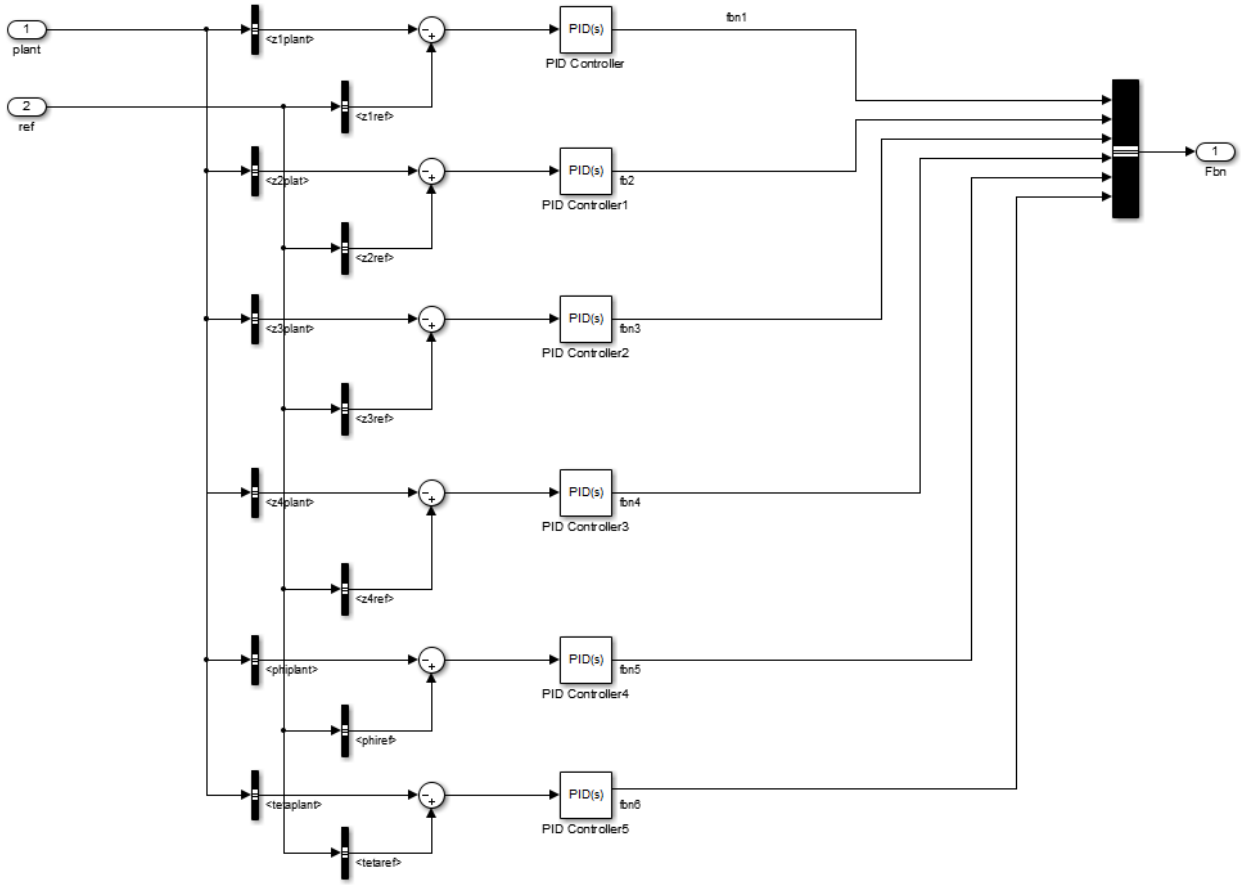

Fig. 38. Block diagram of the suspension system using a PID controller.

When comparing the controlled responses of functions Z_1, $Z_2' - Z_2$, $Z_3' - Z_3$, $Z_4' - Z_4$, φ and θ, utilizing hyperbolic tangent activation functions in the hidden and output layers, with the controlled responses employing hyperbolic tangent in the hidden layer and linear activation in the output layer, it is evident that the neural network in the former state approximates and tracks the control reference input with less error than the latter. Consequently, changing the activation function of the output layer from linear (purelin) to nonlinear (such as hyperbolic tangent or hyperbolic logarithm) does not significantly reduce the approximation error and enhance tracking. Based on the simulation results, the optimal choice for the activation functions of the designed neural network is the nonlinear hyperbolic tangent function (tansig) for the hidden layer and the linear function (purelin) for the output layer. Subsequently, we will implement control actions using a PID controller for the active suspension system of the car, represented by the block diagram in the figure below.

The results of the simulation of the control of the car's active suspension system against the unevenness profile of the road using the PID control system can be seen in the figures below.

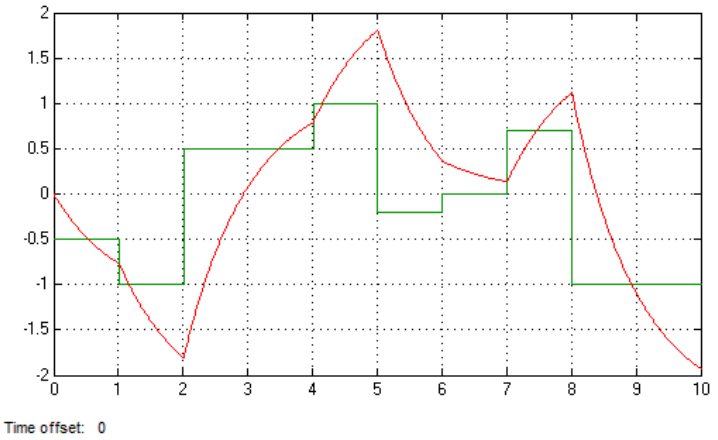

Fig. 39. Controlled response of $Z_1' - Z_1$ function using a PID controller.

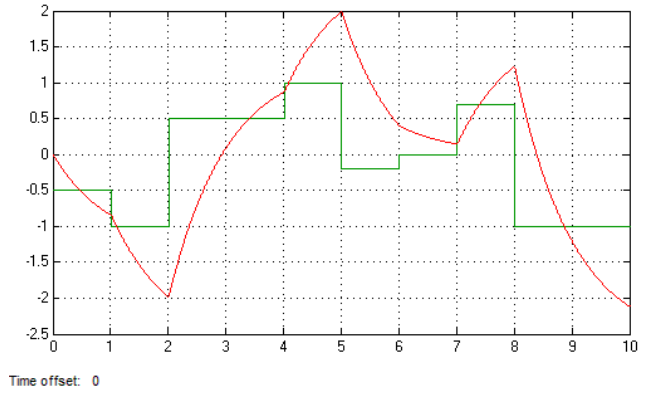

Fig. 40. Controlled response of $Z_2' - Z_2$ function using a PID controller.

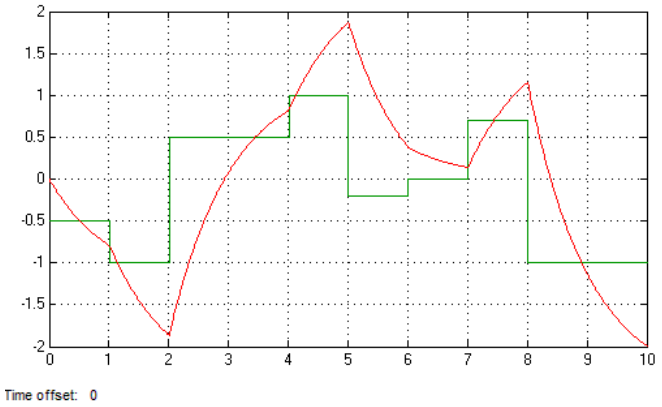

Fig. 41. Controlled response of $Z_3' - Z_3$ function using a PID controller.

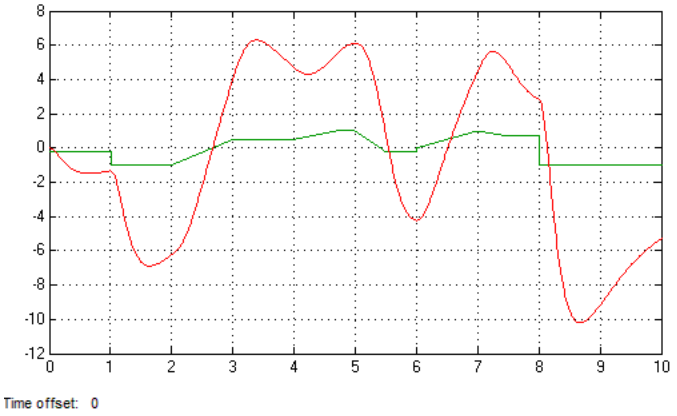

Fig. 42. Controlled response of $Z_4' - Z_4$ function using a PID controller.

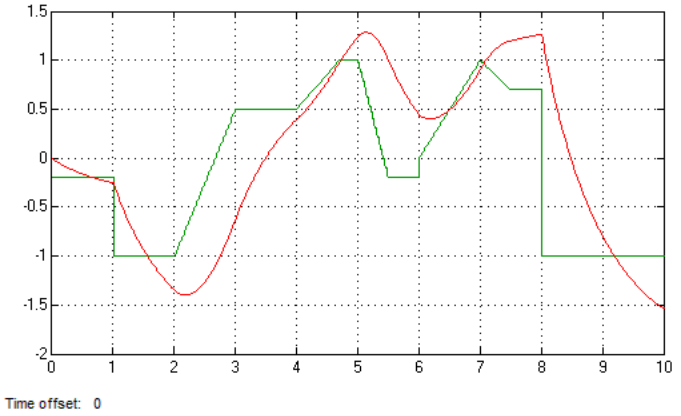

Fig. 43. Controlled response of φ function using a PID controller.

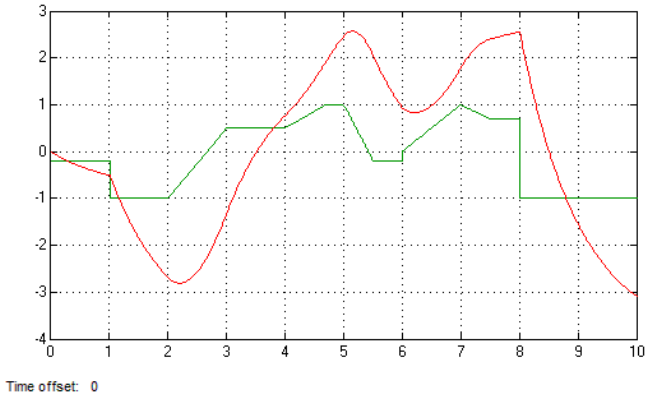

Fig. 44. Controlled response of θ function using a PID controller

The simulation results indicate a substantial disparity and error between the outcomes achieved with the PID controller and the desired control values. Consequently, it is apparent that the PID controller is not well-suited for optimal tracking. In contrast, the robust neural network controller emerges as the superior choice for achieving optimal performance in the active suspension system of the car.

6. CONCLUSION

In this project, a sophisticated neural network-based control system is devised for the comprehensive adjustment of parameters within the active suspension system of the entire vehicle. The complete vehicle model incorporates 7 degrees of freedom. The efficacy of the integrated proportional control system and the proposed robust neural network control system is scrutinized and compared in the context of random road unevenness profiles. The neural network-based control system comprises a robust feedback controller and a predictive controller utilizing a feed-forward neural network. Simulation results affirm that the hybrid control system, integrating a robust feedback controller with a high-performing neural network controller, effectively tracks random road irregularities, underscoring the proposed system's performance, efficiency, and consistency.

A comparative analysis of controlled responses for functions $Z_1' - Z_1$ ،$Z_2' - Z_2$ ،$Z_3' - Z_3$ ،$Z_4' - Z_4$, φ, and θ reveals notable differences between two cases. Specifically, the use of nonlinear activation functions, such as hyperbolic tangent and logarithmic hyperbolic, in the hidden layer is contrasted. The results indicate that employing the hyperbolic tangent function as the activation function in the hidden layer yields better approximation by the neural network and reduces the tracking error of the control reference. Hence, for enhanced performance and minimized tracking errors, it is recommended to adopt the hyperbolic tangent nonlinear function as the activation function in the hidden layer.

Comparing the controlled responses of functions $Z_1' - Z_1$ ،$Z_2' - Z_2$ ،$Z_3' - Z_3$ ،$Z_4' - Z_4$, φ and θ using hyperbolic tangent activation functions in both hidden and output layers with the controlled response obtained by using hyperbolic tangent in the hidden layer and linear activation in the output layer reveals that the neural network in the former case approximates the control reference input with less error than in the latter case. Consequently, altering the activation function of the output layer from the linear function (purelin) to the nonlinear function of the hyperbolic tangent, or even the nonlinear function of the hyperbolic logarithm, does not effectively reduce the approximation error or enhance tracking. Based on comprehensive simulation results, it can be asserted that the optimal choice for activation functions in the designed neural network is the nonlinear hyperbolic tangent function (tansig) for the hidden layer and the linear function (purelin) for the output layer.

Declaration

We acknowledge that we used ChatGPT to enhance the academic writing of our manuscript while ensuring the originality and integrity of our work.

Transparency Statement

The data supporting this study are available upon reasonable request to the corresponding author, subject to ethical and confidentiality considerations.

Acknowledgments

We would like to express our gratitude to all individuals who contributed to this project.

Declaration of Interest

The authors declare that they have no competing interests.

Funding

This research received no specific grant from any funding agency, commercial, or not-for-profit sectors.

REFERENCES

[1] Liu, L., Li, X., Liu, Y., & Tong, S. (2021). Neural network based adaptive event trigger control for a class of

electromagnetic suspension systems. Control Engineering Practice, 106, 104675. https://doi.org/10.1016/j.conengprac.2020.104675

[2] Li, M., Li, J., Li, G., & Xu, J. (2022). Analysis of active suspension control based on improved fuzzy neural network PID. World Electric Vehicle Journal, 13(12), 226. https://doi.org/10.3390/wevj13120226

[3] Liu, Y., Zeng, Q., Liu, L., & Tong, S. (2020). An adaptive neural network controller for active suspension systems with hydraulic actuator. IEEE Transactions on Systems, Man, and Cybernetics: Systems, 50(2), 5351–5360. https://doi.org/10.1109/TSMC.2018.2875187

[4] Swevers, J., Lauwerys, C., Vandersmissen, B., Maes, M., Reybrouck, K., & Sas, P. (2007). A model-free control structure for the online tuning of the semi-active suspension of a passenger car. Mechanical Systems and Signal Processing, 21(3), 1422–1436. https://doi.org/10.1016/j.ymssp.2006.05.005

[5] Gao, H., Lam, J., & Wang, C. (2006). Multi-objective control of vehicle active suspension systems via load-dependent controllers. Journal of Sound and Vibration, 290(3–5), 654–675. https://doi.org/10.1016/j.jsv.2005.04.007

[6] Du, H., & Zhang, N. (2007). H∞ control of active vehicle suspensions with actuator time delay. Journal of Sound and Vibration, 301(1–2), 236–252. https://doi.org/10.1016/j.jsv.2006.09.022

[7] Du, H., Lam, J., & Sze, K. Y. (2003). Non-fragile output feedback H∞ vehicle suspension control using genetic algorithm. Engineering Applications of Artificial Intelligence, 16(7–8), 667–680. https://doi.org/10.1016/j.engappai.2003.09.008

[8] Huang, S. J., & Chen, H. Y. (2006). Adaptive sliding controller with self-tuning fuzzy compensation for vehicle suspension control. Mechatronics, 16(10), 607–622. https://doi.org/10.1016/j.mechatronics.2006.06.002

[9] Ieluzzi, M., Turco, P., & Montiglio, M. (2006). Development of a heavy truck semi-active suspension control. Control Engineering Practice, 14(3), 305–312. https://doi.org/10.1016/j.conengprac.2005.03.019

[10] Thompson, A. G., & Davis, B. R. (2005). Computation of the RMS state variables and control forces in a half-car model with preview active suspension using spectral decomposition methods. Journal of Sound and Vibration, 285(3), 571–583. https://doi.org/10.1016/j.jsv.2004.08.017

[11] Guclu, R. (2005). Fuzzy logic control of seat vibrations of a non-linear full vehicle model. Nonlinear Dynamics, 40, 21–34. https://doi.org/10.1007/s11071-005-3815-7

[12] He, Y., & McPhee, J. (2005). Multidisciplinary design optimization of mechatronic vehicles with active suspensions. Journal of Sound and Vibration, 283(1–2), 217–241. https://doi.org/10.1016/j.jsv.2004.04.027

[13] Guclu, R., & Gulez, K. (2008). Neural network control of seat vibrations of a non-linear full vehicle model using PMSM. Mathematical and Computer Modelling, 47(11–12), 1356–1371. https://doi.org/10.1016/j.mcm.2007.08.013

[14] Yıldırım, S., & Uzmay, I. (2003). Neural network applications to vehicle's vibration analysis. Mechanism and Machine Theory, 38(1), 27–41. https://doi.org/10.1016/S0094-114X(02)00092-7

[15] Anthonis, J., & Ramon, H. (2003). Design of an active suspension to suppress the horizontal vibrations of a spray boom. Journal of Sound and Vibration, 266(3), 573–583. https://doi.org/10.1016/S0022-460X(03)00585-6

[16] Yao, G. Z., Yap, F. F., Chen, G., Li, W. H., & Yeo, S. H. (2001). MR damper and its application for semi-

active control of vehicle suspension system. Mechatronics, 12(8), 963–973. https://doi.org/10.1016/S0957-4158(01)00032-0

[17] Spentzas, K., & Kanarachos, S. A. (2001). Design of a non-linear hybrid car suspension system using neural networks. Mathematics and Computers in Simulation, 60(3–5), 369–378. https://doi.org/10.1016/S0378-4754(02)00029-0

[18] D'Amato, F. J., & Viassolo, D. E. (2000). Fuzzy control for active suspensions. Mechatronics, 10(8), 897–920. https://doi.org/10.1016/S0957-4158(99)00079-3

[19] Yagiz, N., & Yuksek, I. (2001). Sliding mode control of active suspensions for a full vehicle model. International Journal of Vehicle Design, 26(3), 264–276. https://doi.org/10.1504/IJVD.2001.001943

[20] Dayhoff, J. E. (1990). Neural network principles. Prentice-Hall International.

[21] Khanna, T. (1990). Foundations of neural networks. Addison-Wesley Publishing Company.

[22] Fu, B., Giossi, R. L., Persson, R., Stichel, S., Bruni, S., & Goodall, R. (2020). Active suspension in railway vehicles: A literature survey. Railway Engineering Science, 28, 3–35. https://doi.org/10.1007/s40534-020-00207-w